Marcus Cross-Relationship Probed by Time-Resolved CIDNP

Maksim Geniman , Olga B. Morozova , Nikita N. Lukzen , Günter Grampp , Alexandra Yurkovskaya *

Posted Date: 10 August 2023

doi: 10.20944/preprints202308.0868.v1

Keywords: Chemically induced nuclear polarization (CIDNP); guanosine monophosphate; tyrosine anion; short-lived radicals; degenerate electronic exchange; Marcus theory

Article

Marcus Cross-Relationship Probed by Time-Resolved CIDNP

Maksim P. Geniman [1,2], Olga B. Morozova [1], Nikita N. Lukzen [1,2], Günter Grampp [3] and Alexandra V. Yurkovskaya[1,2,*]

[1] International Tomography Center SB RAS, 630090, Novosibirsk, Russia
[2] Novosibirsk State University, 630090, Novosibirsk, Russia
[3] Graz University of Technology, Institute of Physical and Theoretical Chemistry, Stremayrgasse, 9, Graz, Austria grampp@tugraz.at
* Correspondence: yurk@tomo.nsc.ru, +7-905-934-09-29

Abstract: The time-resolved CIDNP method can provide information about degenerate exchange reactions (DEE) involving short-lived radicals. In the temperature range from 8 to 65°C, the DEE reactions of the guanosine-5′-monophosphate anion GMP(-H)$^-$ with the neutral radical GMP(-H)$^\bullet$, of the N-acetyl tyrosine anion NacTyrO$^-$ with a neutral radical NacTyrO$^\bullet$ and of the tyrosine anion TyrO$^-$ with a neutral radical TyrO$^\bullet$ were studied. In all the studied cases, the radicals were formed in the reaction of quenching triplet 2,2′-dipyridyl. The reorganization energies were obtained from Arrhenius plots. The rate constant of the reductive electron-transfer reaction in pair GMP(-H)$^\bullet$/TyrO$^-$ was determined at T = 25°C. Rate constants of GMP(-H)$^\bullet$ radical reduction reactions with TyrO$^-$ and NacTyrO$^-$ anions calculated by the Marcus cross relation differ from the experimental ones by two orders of magnitude. The rate constants of several other electron transfer reactions involving GMP(-H)$^{-/\bullet}$, NacTyrO$^{-/\bullet}$, and TyrO$^{-/\bullet}$ pairs calculated by cross relation agree well with the experimental values. The rate of nuclear paramagnetic relaxation was found for the 3,5 and β-protons TyrO$^\bullet$ and NacTyrO$^\bullet$, the 8-proton GMP(-H)$^\bullet$ the 3,4-protons DPH$^\bullet$ at each temperature. In all cases, the dependences of the rate of nuclear paramagnetic relaxation on temperature are described by the Arrhenius dependence.

Keywords: chemically induced nuclear polarization (CIDNP); guanosine monophosphate; tyrosine anion ; short-lived radicals; degenerate electronic exchange; Marcus theory

1. Introduction

The kinetics of electron transfer reactions is described by Marcus' theory [1]. According to this theory, the rate constant of the electron transfer reaction is expressed as follows:

$$k_{12} = A_{12}\exp\left(-\frac{(\lambda+\Delta G^\circ)}{4\lambda RT}\right) \quad (1)$$

where λ is the reorganization energy, ΔG° is the driving force of the reaction.

The electron transfer reaction is called degenerate if the donor and acceptor differ by only one electron. Degenerate reactions of electron exchange constitute a special section of Marcus theory because the rate constant k_{12} and the reorganization energy λ_{12} of an arbitrary electron transfer reaction can be estimated through the equilibrium constant of the cross-reaction K_{12} and the rate constants k_{11}, k_{22} and the reorganization energies λ_{11}, λ_{22} of the corresponding degenerate electron exchange (DEE) reactions [1]:

$$\lambda_{12} = \frac{\lambda_{11}+\lambda_{22}}{2} \quad (2)$$

$$k_{12} = \sqrt{k_{11}k_{22}K_{12}f_{12}} \quad (3)$$

$$\ln(f_{12}) = \frac{\ln^2(K_{12})}{4\ln\left(\frac{k_{11}k_{22}}{A_{11}A_{22}}\right)} \quad (4)$$

where A_{11}, A_{22} are the pre-exponents of the DEE rate constants. If both reactants are charged, the terms should be added to the equations 3-4 to account for the work of bringing the charged particles closer together.

 doi:10.20944/preprints202308.0868.v1

Equations 2-4 are used to estimate the DEE rate constants if the cross-reaction rate constant and one of the DEE rate constants are known [2-4]. When the rate constants are known only at a single temperature then $A_{11} = A_{22} = 10^{11}$ $M^{-1}s^{-1}$ is often assumed, that introduce an error in the value being determined.

The purpose of this work is to probe the applicability of the Marcus cross-relation with the better accuracy that is provided by knowing of the temperature dependences of the corresponding DEE rate constants. In this case the value of the rate constant of reductive electron transfer to short-lived radical calculated from the cross-relation does not contain the errors due to the uncertainty of the pre-exponent values of the DEE rate constants, since the latter are determined from the temperature dependences of the rates.

To test the Marcus cross-relation, we chose the reduction reactions of the short-lived GMP(-H)$^{\bullet}$ radical by tyrosine ($TyrO^-$) and N-acetyl tyrosine ($NacTyrO^-$) anions. The DEE reactions cannot be studied using optical methods, since there is no change of reactants concentration in course of the reaction, thus the total optical density does not change. The methods for studying DEE reactions between stable reactants (transition metal complexes in different oxidation states, long-lived radicals with the corresponding diamagnetic molecules) usually employ modification one of the reactants. Such methods include the use of deuterated ligands [5], optical isomers [6], and radioactive isotopes [7]. All these methods are not suitable for studying DEE involving short-lived radicals. The DEE reactions between stable reagents can also be studied using line broadening in EPR spectrum [8-11] or in NMR spectra [12-14]. These methods are also not applicable to short-lived radicals, when the lifetime of the radicals is so short that it is impossible to record their EPR or NMR spectra under normal conditions.

The photoinduced time-resolved chemical induced nuclear polarization (tr-CIDNP) method [15-23] fortunately allows to study degenerate exchange reactions involving short-lived radical intermediates [24-26]. It is an indirect way of radical intermediates detection that are formed by short laser pulse via quantitative analysis of anomalous enhancement or emission of NMR lines of the diamagnetic reaction products and their dependence on time after a laser pulse.

The reduction reaction of the neutral radical GMP(-H)$^{\bullet}$ by the anions of tyrosine $TyrO^-$ and N-acetyltyrosine $NacTyrO^-$, was studied by the tr-CIDNP method; dipyridyl (DP) was used as a dye. The CIDNP kinetics for the systems GMP + DP [27], NacTyrOH + DP [28] and GMP + NacTyrOH + DP [29] were previously studied at t = 25ºC in a wide pH range. The temperature dependence for the DEE rate constant in the $GMPH^+/GMPH^{++\bullet}$ pair was also measured earlier [30]. In the temperature range 8-65ºC we measured the DEE rate constants in the pairs GMP(-H)$^-$/GMP(-H)$^{\bullet}$, $TyrO^-/TyrO^{\bullet}$ and $NacTyrO^-/NacTyrO^{\bullet}$. From these temperature dependences of the rate constants the reorganization energies were determined; and with use of their values and Marcus cross relation, the rate constants of the GMP(-H)$^{\bullet}$ radical reduction reaction by $TyrO^-$ and $NacTyrO^-$ anions were calculated. We compared the calculated rate constants with the measured at t = 25ºC electron transfer reaction rate constant for GMP(-H)$^{\bullet}$ + $TyrO^-$ and the previously determined reaction rate constant for the reactants GMP(-H)$^{\bullet}$ + $NacTyrO^-$ [29].

2. Results

2.1. Mechanism of CIDNP effect

The CIDNP spectra recorded during irradiation of solutions containing DP + GMP(-H)$^-$, DP + $TyrO^-$ with signal attribution are shown in Figure 1. The spectra were recorded with zero delay after the laser pulse, without internal standard, the dependence of water chemical shifts on temperature was used: $\delta(HDO) = 5.060 - 0.0122t + (2.11*10^{-5})t^2$ (t in ºC) [31] to relate the chemical shifts.

Preprints (www.preprints.org) | NOT PEER-REVIEWED | Posted: 10 August 2023 doi:10.20944/preprints202308.0868.v1

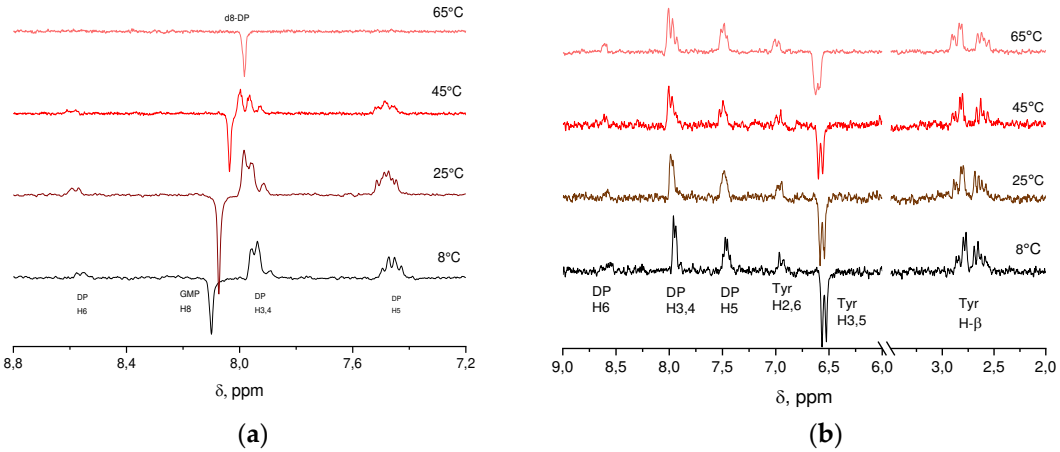

Figure 1. The ^{1}H CIDNP spectra obtained by photo-irradiation of solutions containing a) 15 mM DP and 9, 7.5, 6.5, 4 mM GMP(-H)$^{-}$ at 8, 25, 45, 65ºC and pH = 11.3; b) 15 mM DP and 6.5, 6, 6, 2.5 mM TyrO^{-} at 8, 25, 45, 65ºC and pH = 11.7.

The CIDNP signal origins as follows. The dye molecule D absorbs a quantum of light and transition from the ground singlet state S_0 to the excited singlet state S_1 occurs. Due to inter system crossing (ISC) the S_1 molecule state converts to the triplet electronic state. Then, as a result of diffusion motion, the dye molecule D in the triplet state encounter the quencher Q, which quenches the dye triplet state by means of electron transfer with a rate constant k_q. The radical pair formed in course of this reaction preserves the triplet electron state of the precursor. At the instant of their formation, the radicals are situated in the solvent "cage". They cannot react back to the ground diamagnetic states due to the conservation of the total electron spin. In order for this to happen, the radical pair must change to the singlet state. Such a transition from the triplet to singlet state (and vice versa) can happen due to the difference of Larmor frequencies of the radicals in the field of the NMR spectrometer (at different g- factors) and due to hyperfine couplings of electron spins of the radicals with magnetic nuclei. Thus, in the high field of NMR spectrometer the rate of singlet-triplet transitions depends, besides of g-factor difference, on the nuclear spin projections along the magnetic field, configuration of nuclei spins (S-T_0 mechanism of CIDNP formation in strong magnetic fields). Therefore, the in-cage, geminate, recombination products are enriched in those nuclear spin states that have a higher singlet-triplet interconversion rate. However, the total polarization of nuclear spins does not change since the geminate reaction gives rise only to the sorting between the nuclear polarization of geminate diamagnetic products and the polarization of the radicals which escaped into the bulk of solution. Consequently, at the initial instant of time (on the scale of T_1 nuclear relaxation time in radicals) the nuclear polarization of radicals escaped in the bulk of solution is equal in magnitude and opposite in sign to the polarization of diamagnetic products formed in the course of geminate recombination.

The sign of CIDNP signal Γ of geminate diamagnetic products is determined by the Kaptein rule [32] $\Gamma = \mu \bullet sgn(\Delta g) \bullet sgn(A)$, where $\mu = +1$ in the case of a triplet precursor and $\mu = -1$ in the case of a singlet one; sgn(Δg) is the sign of the g-factor difference of the radicals; sgn(A) is the sign of the hfi-coupling constant of the corresponding nucleus. The value of the g-factor of the neutral GMP(-H)$^{\bullet}$ radical is equal to 2.0034 [33], g-factors for the TyrO$^{\bullet}$ and NacTyrO$^{\bullet}$ radicals are 2.0041 [34] and 2.0055 [35], respectively. The sign of the hfi-coupling constant of the H-8 proton of the GMP(-H)$^{\bullet}$ radical is negative [33], for TyrO$^{\bullet}$ and NacTyrO$^{\bullet}$ the sign of the hfi-coupling constants of the H-3,5 protons is also negative, and of the H-2,6,β protons is positive [34, 35]. There are no experimental data for the DPH$^{\bullet}$ radical, the calculated hfi-coupling constants of the H-3,4,5,6 protons are negative [32], and the value of the g-factor of the DP$^{-\bullet}$ radical anion is equal to 2.0030 [33]. Kaptein's rule holds for all signals in all ^{1}H CIDNP spectra obtained in this work.

2.2. Experimental data processing

Preprints (www.preprints.org) | NOT PEER-REVIEWED | Posted: 10 August 2023 doi:10.20944/preprints202308.0868.v1

Theoretical fitting of the CIDNP kinetics measured for the systems GMP(-H)$^-$ + DP, NacTyrO$^-$ + DP, TyrO$^-$ + DP was performed within the Fisher model [36]. The model takes into account the nuclear polarization transfer from radical into diamagnetic molecule due to the second-order radical recombination, paramagnetic nuclear relaxation in radicals, arising of polarization within re-contacts of radicals in the bulk, and polarization transfer from radical to molecule as a result of DEE. The system of three Eqns. (5-7) describes the time evolution of the radical pair concentration R(t), the nuclear polarization in radicals $P_R(t)$, and the experimentally registered nuclear polarization in diamagnetic molecules $P_{Pr}(t)$:

$$R(t) = \frac{R_0}{1+k_R R_0 t} \quad (5)$$

$$\frac{dP_R(t)}{dt} = -k_R R(t) P_R(t) - k_R \beta R^2(t) - k_{obs} C_q P_R(t) - \frac{P_R(t)}{T_1} \quad (6)$$

$$\frac{dP_{Pr}(t)}{dt} = k_R R(t) P_R(t) + k_R \beta R^2(t) + k_{obs} C_q P_R(t) \quad (7)$$

with initial condition: $P_{Pr}(t=0) = -P_R(t=0) = P_G$.

here R_0 is the initial concentration of radical pairs; k_R is the rate constant for the second-order radical recombination; T_1 is the nuclear spin relaxation time in radicals; k_{obs} is the rate constant for DEE; C_q is the concentration of diamagnetic quencher molecules; parameter $\beta = \gamma P_G/R_0$ shows the amount of polarization arising in one secondary radical pair (the radical pairs formed by radicals escaped from different geminate pairs, so-called F-pairs); γ is the ratio of CIDNP polarization formed in the secondary radical pair to the polarization in the geminate pair, in the case of a triplet precursor one has $\gamma \approx 3$, usually is taken $\gamma = 2.8$ [27]; P_G is the geminate polarization.

The system of Eqns. (5-7) is written assuming that the fraction of geminate recombination of radical pairs is negligible and that the radical formation due to quenching of the triplet state of the dye occurs instantaneously. Eq. (5) describes the time dependence of the radical concentration, which decreases according to the second-order recombination kinetics. The first terms in Eqns. (6-7) describe transfer of polarization from radicals to diamagnetic molecules due to the recombination of radicals, the third terms in both Eqns. (6-7) describe transfer of polarization from radicals to diamagnetic molecules due to DEE process. The second terms in Eqns. (6-7) describe the polarization forming as a result of radicals encounter in the bulk, i.e. in F-pairs. The fourth term in Eq. (6) describes the decay of nuclear polarization in radicals as a result of nuclear paramagnetic relaxation.

Under experimental conditions, there is a DPH$^\bullet$/DP pair (pKa(DPH$^\bullet$) > 14, [37]) . The possible electron and proton transfer (PCET) is much slower than the electron transfer and cannot affect the CIDNP kinetics of DP protons. Therefore, when modeling the kinetic curves for nuclear polarization of DP, we took $k_{obs} = 0$.

In the system GMP(-H)$^-$ + TyrO$^-$ + DP, the kinetics of nuclear polarization is also affected by the reduction reaction of the GMP(-H)$^\bullet$ radical by the TyrO$^-$ anion. Then, the time evolution of the concentrations of GMP(-H)$^\bullet$, TyrO$^\bullet$ and DPH$^\bullet$ radicals and the polarizations of the nuclei in P_R^{GMP}, P_R^{Tyr} radicals, and P_{Pr}^{GMP}, P_{Pr}^{Tyr} diamagnetic molecules are described by the following equations:

$$\frac{dR^{Tyr}}{dt} = -k_R^{TYR} R^{Tyr} R^{DP} + k_{obs}^{red} R^{GMP} C^{Tyr} \quad (8)$$

$$\frac{dR^{GMP}}{dt} = -k_R^{GMP} R^{GMP} R^{DP} - k_{obs}^{red} R^{GMP} C^{Tyr} \quad (9)$$

$$R^{DP} = R^{GMP} + R^{Tyr} \quad (10)$$

$$\frac{dP_R^{GMP}}{dt} = -k_R^{GMP} R^{DP} P_R^{GMP} - k_R^{GMP} \beta^{GMP} R^{DP} R^{GMP} - k_{obs}^{GMP} C^{GMP} P_R^{GMP} - k_{obs}^{red} P_R^{GMP} C^{Tyr} - \frac{P_R^{GMP}}{T_1^{GMP}} \quad (11)$$

$$\frac{dP_{Pr}^{GMP}}{dt} = k_R^{GMP} R^{DP} P_R^{GMP} + k_R^{GMP} \beta^{GMP} R^{DP} R^{GMP} + k_{obs}^{GMP} C^{GMP} P_R^{GMP} + k_{obs}^{red} P_R^{GMP} C^{Tyr} \quad (12)$$

$$\frac{dP_R^{Tyr}}{dt} = -k_R^{Tyr} R^{DP} P_R^{Tyr} - k_R^{Tyr} \beta^{Tyr} R^{DP} R^{Tyr} - k_{obs}^{Tyr} C^{Tyr} P_R^{Tyr} - \frac{P_R^{Tyr}}{T_1^{Tyr}} \quad (13)$$

$$\frac{dP_{Pr}^{Tyr}}{dt} = k_R^{Tyr} R^{DP} P_R^{Tyr} + k_R^{Tyr} \beta^{Tyr} R^{DP} R^{Tyr} + k_{obs}^{Tyr} C^{Tyr} P_R^{Tyr} \quad (14)$$

with initial conditions: $P_{Pr}^{GMP}(t=0) = -P_R^{GMP}(t=0) = P_G^{GMP}$, $P_{Pr}^{Tyr}(t=0) = -P_R^{Tyr}(t=0) = P_G^{Tyr}$, here k_R^{GMP}, k_R^{Tyr} are the recombination rate constants of the radicals DPH$^\bullet$ with GMP(-H)$^\bullet$ and TyrO$^\bullet$ radicals respectively, k_{obs}^{red} is the observed rate constant of reduction of the GMP(-H)$^\bullet$ radical by tyrosinate-anion, $\beta^{GMP} = \gamma P_G^{GMP}/R_0^{GMP}$, $\beta^{Tyr} = \gamma P_G^{Tyr}/R_0^{Tyr}$.

Preprints (www.preprints.org) | NOT PEER-REVIEWED | Posted: 10 August 2023 doi:10.20944/preprints202308.0868.v1

In the process of solving this system of equations, the parameters k_R^{GMP}/k_R^{Tyr} and k_q^{GMP}/k_q^{Tyr} are introduced, through the latter the ratio of initial concentrations of GMP(-H)• and TyrO• radicals is expressed.

The initial concentration of radical pairs R_0 is proportional to the fraction of light absorbed by the dye. The $TyrO^-$, $NacTyrO^-$ compounds absorb at λ = 308 nm, as the concentration of tyrosine in the solution increases, the fraction of light absorbed by DP decreases and, accordingly, the initial concentration of radical pairs decreases as well. The ratio of initial concentrations of radical pairs in two experiments with different concentrations of tyrosine is as follows:

$$\frac{R_0\left(C_1^{Tyr}\right)}{R_0\left(C_2^{Tyr}\right)} = \frac{\varepsilon^{DP}C^{DP}+\varepsilon^{Tyr}C_2^{Tyr}}{\varepsilon^{DP}C^{DP}+\varepsilon^{Tyr}C_1^{Tyr}} \quad (15)$$

In Eq. (15) ε^{DP}, ε^{Tyr} are the extinction coefficients at λ = 308 nm; C^{DP} is DP concentration; C_1^{Tyr}, C_2^{Tyr} are tyrosine concentrations; $\varepsilon^{DP} = 1.2*10^3$ $M^{-1}cm^{-1}$ [38], $\varepsilon^{TyrO^-} = \varepsilon^{NacTyrO^-} = 790\pm8$ $M^{-1}cm^{-1}$ was determined in this work. This effect was taken into account when modeling CIDNP kinetics in systems containing $TyrO^-$ and $NacTyrO^-$.

The duration of the RF pulse (1-2 μs) is comparable with the characteristic time of the CIDNP decay, so it is necessary to take into account the polarization evolution during the RF pulse. Consideration of the CIDNP kinetics during the RF pulse for the special case of an ideal rectangular pulse is considered in [39], the case of an RF pulse of arbitrary shape is considered in [40]. The similar approach was used in the works of Morozova and Yurkovskaya [41-48].

To take into account the CIDNP kinetics during the application of the RF pulse along the x-axis, we considered the following system of equations that takes into account the polarization of the nuclei along the y, z axes:

$$\frac{dP_{Pr}^z}{dt} = \frac{dP_{Pr}}{dt} - w(t)P_{Pr}^y \quad (16)$$

$$\frac{dP_{Pr}^y}{dt} = w(t)P_{Pr}^z \quad (17)$$

where w(t) is the pulse shape, the equation for dP_{Pr}/dt is given by Eq. (7), before the pulse P_{Pr}^y = 0. The signal observed in the experiment is proportional to the after pulse value of P_{Pr}^y. The expression for polarization along the y-axis after the pulse is as follows [39]:

$$P_{Pr}^y = \int_0^T P_{Pr}(t_0+t)w(t)\cos\left(\int_t^T w(z)dz\right)dt \quad (18)$$

where t_0 is the start time of the RF pulse, T is its duration.

The duration of the π pulse is equal to t_π = 12.70 μs. The shapes of RF pulses of 1 and 2 μs duration used in this work were determined using an oscilloscope.

2.3. Results of CIDNP kinetics treatment

In the $GMP(-H)^-$ + DP system, the polarization-time dependences were modeled for 8-th GMP protons and 3,4 DP protons. In the $TyrO^-$ + DP, $NacTyrO^-$ + DP systems, the dependences were modeled for 3,5 and β-protons of tyrosine, and 3,4 protons of DP – the other signals have too low signal-to-noise ratio. In the $GMP(-H)^-$ + $TyrO^-$ + DP system, CIDNP polarization time dependences were modeled for 8-th GMP protons and 3,5 tyrosine protons. Values of the degenerate electron exchange rate constants and paramagnetic nuclear relaxation times obtained from the best agreement between the calculated and experimental curves are given in Tables 1–3; Figure 2(a-c) shows the examples of simulations of these experimental data.

Table 1. Fitting parameters for the $GMP(-H)^-$ + DP system.

t°C	k_{obs}, $M^{-1}s^{-1}$	$T_1(H_8)$, μs	$T_1(H_{3,4}$ DP), μs	k_{et}, $M^{-1}s^{-1}$
8	$(3.77\pm0.11)*10^7$	12.4±0.5	49±8	$(4.27\pm0.14)*10^7$
25	$(4.91\pm0.27)*10^7$	20.4±1.6	60±10	$(5.50\pm0.32)*10^7$
45	$(5.78\pm0.28)*10^7$	26.1±2.2	121±34	$(6.32\pm0.32)*10^7$
65	$(8.12\pm0.38)*10^7$	55±13	-- (d8-DP)	$(9.04\pm0.45)*10^7$

Table 2. Fitting parameters for the $NacTyrO^-$ + DP system.

Preprints (www.preprints.org) | NOT PEER-REVIEWED | Posted: 10 August 2023 doi:10.20944/preprints202308.0868.v1

t°C	k_{obs}, $M^{-1}s^{-1}$	$T_1(H_{3,5})$, μs	$T_1(H_\beta)$, μs	$T_1(H_{3,4}$ DP), μs	k_{et}, $M^{-1}s^{-1}$
8	$(4.46\pm0.09)*10^7$	34.5±2.3	111±16	51.1±7	$(4.71\pm0.10)*10^7$
25	$(5.07\pm0.18)*10^7$	58±7	119±24	69.1±15	$(5.27\pm0.19)*10^7$
45	$(6.95\pm0.22)*10^7$	75±13	129±35	73.2±24	$(7.19\pm0.23)*10^7$
65	$(8.24\pm0.57)*10^7$	50±9	--	42.1±19	$(8.46\pm0.60)*10^7$

Table 3. Fitting parameters for the $TyrO^-$ + DP system.

t°C	k_{obs}, $M^{-1}s^{-1}$	$T_1(H_{3,5})$, μs	$T_1(H_\beta)$, μs	$T_1(H_{3,4}$ DP), μs	k_{et}, $M^{-1}s^{-1}$
8	$(2.81\pm0.13)*10^7$	41.1±3	118±25	98±22	$(2.94\pm0.14)*10^7$
15	$(3.59\pm0.28)*10^7$	45±6	138±21	54±10	$(3.76\pm0.30)*10^7$
25	$(4.78\pm0.27)*10^7$	50±7	139±26	199±81	$(5.02\pm0.29)*10^7$
35	$(5.64\pm0.36)*10^7$	63±11	149±36	95±32	$(5.90\pm0.39)*10^7$
45	$(5.96\pm0.42)*10^7$	82±19	--	137±35	$(6.19\pm0.45)*10^7$
55	$(7.60\pm0.37)*10^7$	56±10	121±32	48±16	$(7.92\pm0.40)*10^7$
65	$(8.53\pm0.49)*10^7$	65±14	106±30	67±22	$(8.87\pm0.52)*10^7$

For the $GMP(-H)^-$ + DP we did not determine T1 for 3,4 protons of DP at 65°C because perdeuterated d8-DP was used due to the overlapping the ^1H NMR signals of H-8 of GMP and H-3,4 of DP. For $NacTyrO^-$ + DP at 65°C and $TyrO^-$ + DP at 45°C we failed to determine T_1 for H-β.

For $GMP(-H)^-$ + DP at 25ºC, the value of the DEE rate constant differs from the literature data, while the paramagnetic relaxation time of the 8-th proton in the GMP(-H)• radical coincides well with the literature data: $k_{obs} = 4.0*10^7$ $M^{-1}s^{-1}$, T_1 =20 μs [27]. Moreover, the T_1 for the 8-th proton in the GMP(-H)• radical coincides with the previously found T_1 for the 8-th proton in the $GMPH^{+\bullet}$ radical over the entire temperature range [30]. For the $NacTyrO^-$ + DP at t = 25ºC the values of the DEE rate constant and paramagnetic relaxation time of 3,5 protons coincide with the literature data: k_{obs} = $6.0*10^7$ $M^{-1}s^{-1}$, T_1 =63 μs [29]; = $4*10^7$ $M^{-1}s^{-1}$, T_1 = 60 μs [49]. However, the best fit values of nuclear paramagnetic relaxation times for 3,4 protons in the DPH• radical do not coincide with the literature data T_1 = 44 μs [28, 38, 50] and T_1 = 45 μs [49].

Simulation of the experimental data for DP + $GMP(-H)^-$ + $TyrO^-$ is shown in Figure 2-d, the parameters found are: $k_{obs}^{red} = 1.5*10^8$ $M^{-1}s^{-1}$, $k_q^{GMP}/k_q^{Tyr} = 0.3$, $k_R^{GMP}/k_R^{Tyr} = 1.3$. The parameters k_{obs}^{GMP}, k_{obs}^{Tyr}, T_1^{GMP}, and T_1^{Tyr} found in this work were used in the calculation. There are literature data for the reduction of GMP(-H)• radical by $NacTyrO^-$ anion: $k_{obs}^{red} = 1.6*10^8$ $M^{-1}s^{-1}$, $k_q^{GMP}/k_q^{Tyr} = 0.56$, $k_R^{GMP}/k_R^{Tyr} = 0.9$ [29].

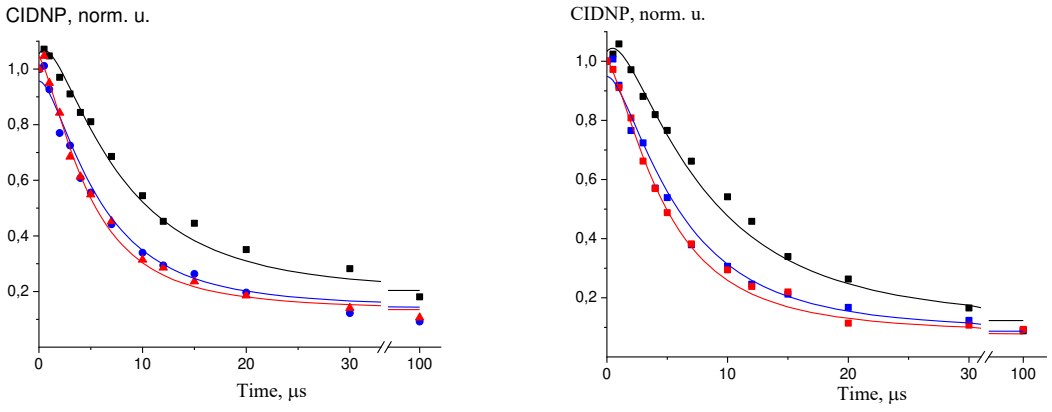

(**a**) (**b**)

Preprints (www.preprints.org) | NOT PEER-REVIEWED | Posted: 10 August 2023 doi:10.20944/preprints202308.0868.v1

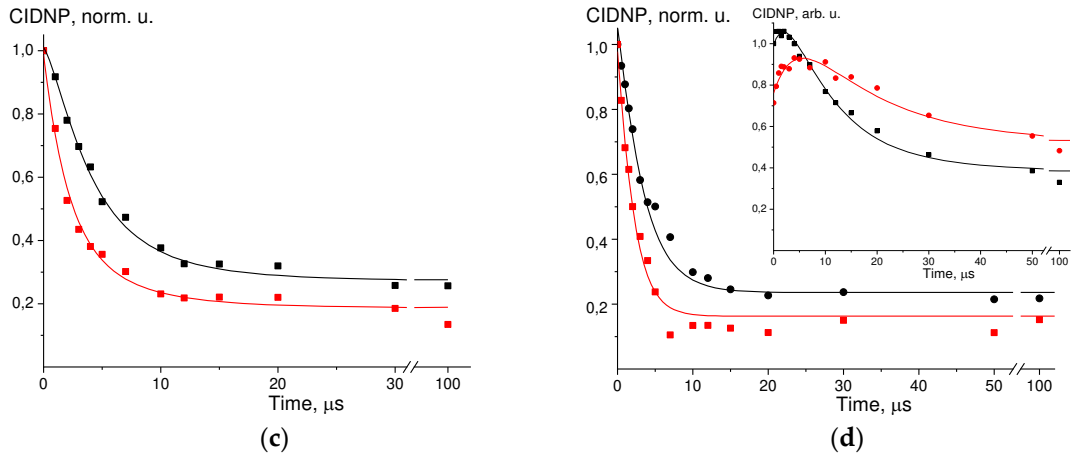

Figure 2. Experimental data (dots) and simulation curves (solid lines) for:.

a) $TyrO^-$ + DP at t = 65°C, kinetics for H-3.5 $TyrO^-$, black – C($TyrO^-$) = 1.5 mM, blue – C($TyrO^-$) = 2.5 mM, red – C($TyrO^-$) = 3.5 mM;.

b) $TyrO^-$ + DP at t = 65°C, kinetics for H-β $TyrO^-$, black – C($TyrO^-$) = 1.5 mM, blue – C($TyrO^-$) = 2.5 mM, red – C($TyrO^-$) = 3.5 mM;.

c) $GMP(-H)^-$ + DP at t = 45°C, kinetics for H-8 $GMP(-H)^-$, black – C(GMP) = 6.5 mM, red – C(GMP) = 13 mM;.

d) $GMP(-H)^-$ + $TyrO^-$ + DP at t = 25ºC, kinetics for H-8 $GMP(-H)^-$, black – C($TyrO^-$) = 1.3 mM, red – C($TyrO^-$) = 2.5 mM, insert – kinetics for H-3.5 $TyrO^-$, black – C($TyrO^-$) = 1.3 mM, red – C($TyrO^-$) = 2.5 mM.

2.4. Temperature dependence of the DEE rate constants

For the estimation of the effect of diffusion the following DEE kinetic scheme was considered (using tyrosine as an example):

$$TyrO^- + TyrO^\bullet \underset{k_{-d}}{\overset{k_d}{\rightleftharpoons}} [TyrO^- + TyrO^\bullet] \underset{w_{ex}}{\overset{w_{ex}}{\rightleftharpoons}} [TyrO^\bullet + TyrO^-] \underset{k_d}{\overset{k_{-d}}{\rightleftharpoons}} TyrO^\bullet + TyrO^-$$

where the first-order DEE rate wex is related to the second-order rate constant k_{et} as:

$$w_{ex} = k_{et}\frac{k_{-d}}{k_d} \quad (19)$$

k_{obs} is the observable DEE rate constant, k_{obs} it is expressed through k_{et} and k_d as follows:

$$k_{obs} = \frac{k_{et}k_d}{2k_{et}+k_d} \quad (20)$$

The diffusion rate constant k_d was estimated by the Smoluchowski equation, taking into account the charges of the reactants:

$$k_d = \frac{2}{3\eta}\cdot\frac{(r_1+r_2)^2}{r_1r_2}\cdot\frac{w_r}{\exp\left(\frac{w_r}{RT}\right)-1} \quad (21)$$

where r_1, r_2 are the radii of the reagents; w_r is the work function of approach charged reactants to each other:

$$w_r = \frac{z_1z_2e^2N_A}{4\pi\varepsilon_0\varepsilon(r_1+r_2)}f \quad (22)$$

we assume that the reactants approaches to the distance equal to the sum of their radii. The factor f takes into account the ionic strength of the solution:

$$f = \left(1+(r_1+r_2)B\sqrt{\frac{\mu}{\varepsilon T}}\right)^{-1} \quad (23)$$

where $B = (2N_Ae^2/(\varepsilon_0 k))^{1/2} = 50.345\ l^{1/2}K^{1/2}Å^{-1}M^{-1/2}$.

Preprints (www.preprints.org) | NOT PEER-REVIEWED | Posted: 10 August 2023 doi:10.20944/preprints202308.0868.v1

The viscosity values of D_2O were taken from [51, 52], dielectric permittivity from [53]. The average elliptical radii of the reactants were used to estimate r_1 and r_2. An ellipsoid of the smallest volume was described around the molecule and the radius was expressed as [54]:

$$\frac{1}{r} = \frac{F(\varphi,\alpha)}{\sqrt{(a^2-c^2)}} \quad (24)$$

where $F(\varphi,\alpha)$ is an elliptic integral of the first kind; $\varphi = \arcsin((a^2 - c^2)^{1/2}/a)$; $\alpha = ((a^2 - c^2)/(a^2 - b^2))^{1/2}$; a, b, c are the semiaxes of the ellipsoid, $a \geq b \geq c$.

The ellipsoid semiaxes were calculated using the algorithm N. Shor [55] with the molecular geometries of the crystal structures of DL-tyrosine [56], N-acetyl-L-tyrosine and guanosine-5'-monophosphate trihydrate [57]. The molecular radii found: r(GMP(-H)$^-$) = 4.18 Å, r(NacTyrO$^-$) = 3.82 Å, r(TyrO$^-$) = 3.06 Å, we assumed that the radii of the radicals do not differ from those of the corresponding diamagnetic particles.

When calculating w_r, the negatively charged carboxyl and phosphate groups in the reactants were taken into account: z(GMP(-H)$^-$) = -3, z(TyrO$^-$) = -2.

The k_{et} values calculated by Eq.(20) are given in the last columns of Table **Error! Reference source not found.-Error! Reference source not found.**.

The first-order DEE rate constant w_{ex} depends on temperature as [1]:

$$w_{ex}(T) = \frac{k_0}{\sqrt{T}} exp\left(-\frac{\lambda}{4RT}\right) \quad (25)$$

The second-order DEE rate constant k_{et} is expressed as follows:

$$k_{et} = \frac{k_d}{k_{-d}} k_{ex} = K_A w_{ex} \quad (26)$$

The K_A in Eq. (26) is the equilibrium constant of pre-reaction complex formation; it depends on temperature as follows [58] :

$$K_A = 4\pi N_A (r_1 + r_2)^2 \delta d \cdot \exp\left(-\frac{w_r}{RT}\right) = K_0 \exp\left(-\frac{w_r}{RT}\right) \quad (27)$$

where δd is the reaction zone thickness. Then the second-order rate constant k_{et} depends on temperature as:

$$k_{et} = \frac{K_0 k_0}{\sqrt{T}} exp\left(-\frac{w_r}{RT} - \frac{\lambda}{4RT}\right) = \frac{A}{\sqrt{T}} exp\left(-\frac{w_r}{RT} - \frac{\lambda}{4RT}\right) \quad (28)$$

The work function w_r depends on the temperature through dependence on temperature of the D_2O dielectric permittivity, at each temperature w_r can be calculated by Eq. (22). To find the pre-exponent A and the reorganization energy λ, we plot the values of $\ln[k_{et}\sqrt{T}\exp(w_r/RT)]$, where the k_{et} values are experimental ones, versus 1/T (Figure 3) and and approximated these points by linear dependence. The values of A and λ found from the approximation are given in Table 4.

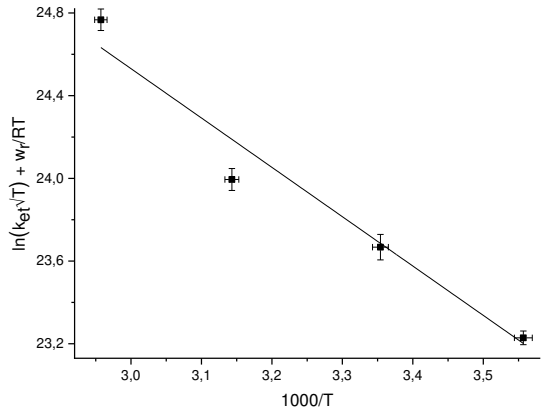

(**a**)

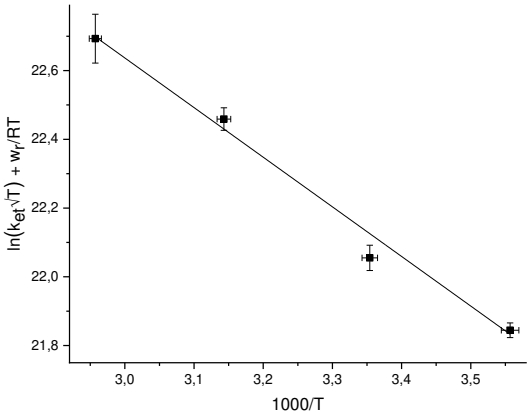

(**b**)

Preprints (www.preprints.org) | NOT PEER-REVIEWED | Posted: 10 August 2023 doi:10.20944/preprints202308.0868.v1

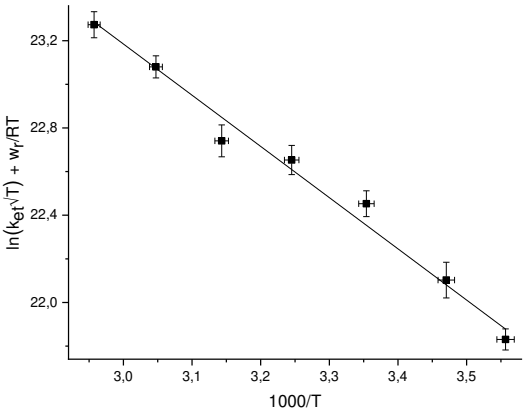

(c)

Figure 3. Temperature dependences of the DEE rate constants ket in the coordinates $\ln[k_{et}\sqrt{T}\exp(w_r/RT)]$ vs 1/T for: a) GMP(-H)• + GMP(-H)$^-$ b) NacTyrO• + NacTyrO$^-$ c) TyrO• + TyrO-.

Table 4. The found pre-exponents and reorganization energies for DEE reactions.

DEE reaction	ln(A)	λ, eV
GMP(-H)$^-$ + GMP(-H)•	31.7 ± 1.0	0.82 ± 0.11
NacTyrO$^-$ + NacTyrO•	27.0 ± 0.4	0.50 ± 0.04
TyrO$^-$ + TyrO•	30.2 ± 0.4	0.81 ± 0.04

Previously we studied [30] the temperature dependence of the DEE rate constant between the GMPH$^+$ cation and the GMPH$^{++\bullet}$, dication radical, the reorganization energy found for this reaction is λ = 0.79 ± 0.11 eV [21] and coincides with the value for GMP(-H)$^-$ + GMP(-H)• (see Table **Error! Reference source not found.**).

2.5. The Marcus cross-relation equation

To account for the effects of diffusion the following kinetic scheme of electron transfer was considered (for the radical GMP(-H)• reduction by anion TyrO$^-$ as an example):

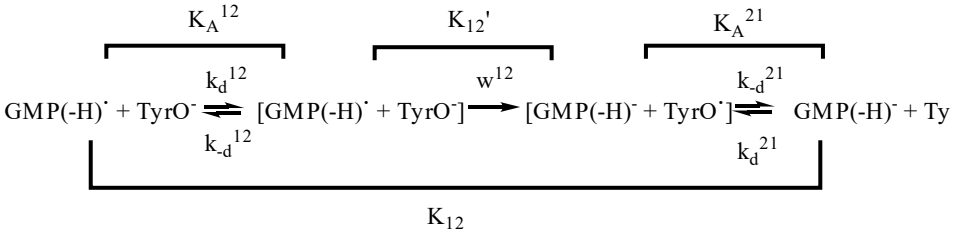

where the first-order rate w^{12} is related to the second-order rate constant k^{12} as:

$$w^{12} = \frac{k_{-d}^{12}}{k_d^{12}} k^{12} \quad (29)$$

The observable second-order rate constant k_{obs}^{12} is expressed through k^{12} and k_d^{12} as follows:

$$k_{obs}^{12} = \frac{k^{12} k_d^{12}}{k^{12} + k_d^{12}} \quad (30)$$

The rate constants k^{12}(TyrO$^-$) and k^{12}(NacTyrO$^-$) of GMP(-H)• reduction by TyrO$^-$ and NacTyrO$^-$ respectively after correction for diffusion (k_d was calculated according Eq. (21)) are the following: k^{12}(TyrO-) = 1.7*10^8 M^{-1}s^{-1} and k^{12}(NacTyrO$^-$) = 1.8*10^8 M^{-1}s^{-1} [29]. Thus, the values of the reduction rate constants are very close.

The rate constant w^{12} depends on the temperature as follows:

$$w^{12} = \frac{k_0}{\sqrt{T}} exp\left(-\frac{(\Delta G_{12}^{0\prime} + \lambda_{12})^2}{4RT\lambda_{12}}\right) \quad (31)$$

where $\Delta G_{12}^{o\prime}$ is the driving force of the first-order redox reaction.

The equilibrium constant between the initial reactants and reaction products K_{12} is expressed as:

$$K_{12} = exp\left(-\frac{\Delta G_{12}^0}{RT}\right) = K_A^{12} K_{12}{}' (K_A^{21})^{-1} = exp\left(\frac{-\Delta G_{12}^{0\prime} - w_{12} + w_{21}}{RT}\right) \quad (32)$$

Preprints (www.preprints.org) | NOT PEER-REVIEWED | Posted: 10 August 2023 doi:10.20944/preprints202308.0868.v1

here K_A^{12} and K_A^{21} are the equilibrium constants of the formation of pre-reaction and post-reaction complexes, expressed by Eq. (27). Assuming the radii of radicals and corresponding diamagnetic particles are the same, the pre-exponents in Eq. (32) the factors K_A^{12} and K_A^{21} can be shortened (reduced). The ΔG_{12}^{o} value is expressed through standard electrode potentials, thus, $\Delta G_{12}^{o'}$ can be calculated.

The expression for the second-order electron transfer rate constant k^{12} is given as follows:

$$k^{12} = K_A^{12} w^{12} = \frac{A_{12}}{\sqrt{T}} exp\left(-\frac{w_{12}}{RT}\right) exp\left(-\frac{\left(\Delta G_{12}^{0} - w_{12} + w_{21} + \lambda_{12}\right)^2}{4RT\lambda_{12}}\right) \quad (33)$$

If the electron transfer occurs over a relatively long distance with a weak force interaction between the reactants, then one can assume that $\lambda_{12} = (\lambda_{11} + \lambda_{22})/2$ that is the Marcus cross relation, where λ_{11}, λ_{22} are the reorganization energies for the respective DEE reactions.

If we additionally assume the following ratio between the pre-exponents: $A_{12} = (A_{11}A_{22})^{1/2}$, then we can express k^{12} through the temperature dependence parameters of the DEE rate constants. Thus, the cross-reaction rate constant k_{calc}^{12} was calculated employing the following formula:

$$k_{calc}^{12} = \frac{\sqrt{A_{11}A_{22}}}{\sqrt{T}} exp\left(-\frac{w_{12}}{RT}\right) exp\left(-\frac{\left(\Delta G_{12}^{0} - w_{12} + w_{21} + (\lambda_{11} + \lambda_{22})/2\right)^2}{2RT(\lambda_{11} + \lambda_{22})}\right) \quad (34)$$

2.5.1. Reactants parameters for the Marcus cross-relation calculations

The cross-relation calculations require the values of the difference of standard electrode potentials, the reorganization energy and the pre-exponent for the corresponding DEE reactions, as well as the radii of all reactants and products to calculate the work function. In all the cases, we assume that the radii of radicals and corresponding diamagnetic particles are the same.

If only the DEE rate constant at a certain temperature is known, we estimate the pre-exponent as: $A_{11} = 10^{11}$ $M^{-1}s^{-1}$ and calculate the reorganization energy by Eq. (35).

$$\lambda_{11} = -4w_r - 4RT * ln\left(\frac{k_{11}\sqrt{T}}{A_{11}}\right) \quad (35)$$

All the parameters of the reactants are given in Table **Error! Reference source not found.**. The Z_{red} column shows the charge of the reduced form of each reactant. The structures of some reactants are shown in Figure 4.

The TyrO•/TyrO$^-$ case. The standard electrode potential is E° = 0.72 V [59]. The radius calculation is described above, the pre-exponent and reorganization energy for the DEE reaction were found experimentally in this work.

The NacTyrO•/NacTyrO$^-$ case. We use the value of the standard electrode potential for N-acetyltyrosine methyl ester at pH = 7, E_7 = 0.97 V [60]. pK_a(NacTyrOH) = 10.1, then E^o = 0.79 V. The calculation of the radius is described above; the pre-exponent and reorganization energy for the DEE reaction were found experimentally in this work.

The GMP(-H)•/GMP(-H)$^-$ case. The standard electrode potential of GMP at pH = 7, E_7 = 1.31 V [61], determined from photoinduced electron transfer reaction rates, that agrees well with that of guanosine at pH = 7, E_7 = 1.29 V [62], determined by pulsed radiolysis. The acidity constants of GMP [63] and its radical [64-66] are shown in Figure **Error! Reference source not found.**. For GMP(-H)•/GMP(-H)$^-$ the calculated potential is: E^o = 1.23 V.

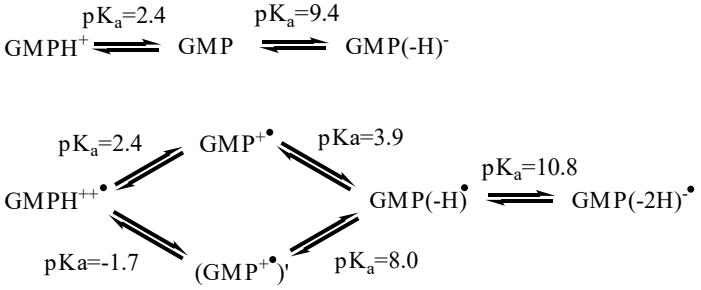

Figure 4. Acid-base equilibria for GMP and radical GMP•.

Preprints (www.preprints.org) | NOT PEER-REVIEWED | Posted: 10 August 2023 doi:10.20944/preprints202308.0868.v1

The $GMPH^{++\bullet}/GMPH^{+}$ case. The standard electrode potential E° = 1.55 V, calculated from E^7 = 1.29 V [62]. The pre-exponent and reorganization energy for the DEE reaction were found earlier [30]. Average elliptical radius r = 4.19 Å, calculated by the method described above, the geometry was taken from the crystal structure of guanosine-5'-monophosphate trihydrate [57]

The $NacTrpH^{+\bullet}/NacTrpH$ case, we use the value of the standard electrode potential for tryptophan, E° = 1.15 V [59]. The DEE rate constant at 25°C is $k_{11} = 9*10^8$ $M^{-1}s^{-1}$ was determined experimentally by CIDNP with microsecond resolution [38]. After correction for diffusion by Eq. (20) one has: $k_{11} = 1.3*10^9$ $M^{-1}s^{-1}$. The mean elliptical radius r = 3.83 Å was calculated by the method described above, geometry from was taken from the NacTrpH crystal structure [67]. We assume that $A_{11}/\sqrt{T} = 10^{11}$ $M^{-1}s^{-1}$, then λ = 0.45 eV.

The $ClO_2^{\bullet}/ClO_2^{-}$ case. The standard electrode potential E° = 0.934 V [68]. The DEE constant at 25°C is $k_{11} = 3.3*10^4$ $M^{-1}s^{-1}$, determined from a cross relation with parameters $A_{11}/\sqrt{T} = 10^{11}$ $M^{-1}s^{-1}$, r = 1.5 Å [69]. Then λ_{11} = 1.53 eV.

The $N_3^{\bullet}/N_3^{-}$ case. The standard electrode potential E° = 1.33 V [68]. The DEE rate constant at 25°C $k_{11} = 3.7*10^6$ $M^{-1}s^{-1}$, determined from a cross relation with parameters $A_{11}/\sqrt{T} = 10^{11}$ $M^{-1}s^{-1}$, r = 2 Å [69]. Then λ_{11} = 1.05 eV.

The $NO_2^{\bullet}/NO_2^{-}$ case. The standard electrode potential E° = 1.04 V [68]. The DEE rate constant at 25°C k_{11} = 580 $M^{-1}s^{-1}$, determined experimentally by isotopic substitution [70]. We assume that $A_{11}/\sqrt{T} = 10^{11}$ $M^{-1}s^{-1}$, then λ = 1.95 eV. The radius r = 1.9 Å [69].

The $[IrCl_6]^{2-}/[IrCl_6]^{3-}$ case. The standard electrode potential E° = 0.892 V [71]. The DEE constant at 25°C $k_{11} = 2.3*10^5$ $M^{-1}s^{-1}$, determined experimentally by isotopic substitution [72]. We assume that $A_{11}/\sqrt{T} = 10^{11}$ $M^{-1}s^{-1}$. Radius r = 4.4 Å [73], DEE rate constant measured at μ = 0.1 M. Then λ = 1.04 eV.

The $CysS^{\bullet}/CysS^{-}$ case. The standard electrode potential E° = 0.76 V [74]. The DEE rate constant at 25°C $k_{11} = 5.4*10^3$ $M^{-1}s^{-1}$, determined from the Marcus cross relation with parameters $A_{11}/\sqrt{T} = 10^{11}$ $M^{-1}s^{-1}$, r = 3.0 Å, the k_{12} cross-reaction rate constant was measured at μ = 0.1 M [74]. Then λ = 1.48 eV.

The $TEMPO^{+}/TEMPO^{\bullet}$ case. The standard electrode potential E° = 0.745 V [75]. The DEE rate constant at 25°C $k_{obs} = 8.6*10^7$ $M^{-1}s^{-1}$, determined experimentally by line broadening in the EPR spectrum [76]. After correction for diffusion by Eq. (20), $k_{11} = 8.8*10^7$ $M^{-1}s^{-1}$. We assume that $A_{11}/\sqrt{T} = 10^{11}$ $M^{-1}s^{-1}$. Then λ = 0.72 eV. The radius r = 3.67 Å [76].

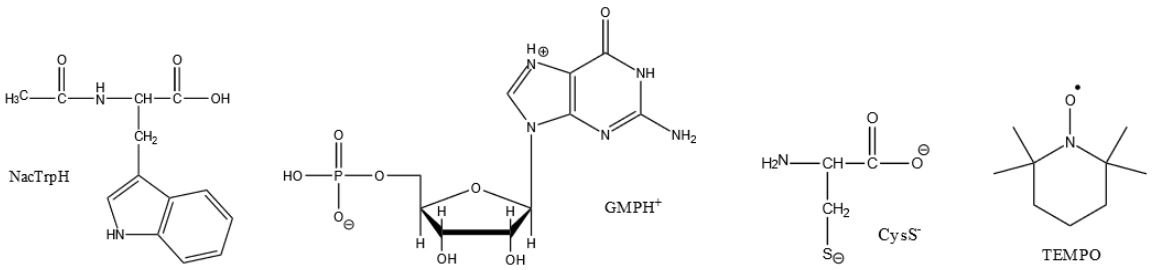

Figure 5. Structures of N-acetyltryptophan (NacTrpH), guanosine-5'-monophosphate cation ($GMPH^{+}$), cysteine anion ($CysS^{-}$), stable free radical TEMPO – (2,2,6,6-tetramethylpiperidin-1-yl)oxyl.

Table 5. Parameters of the reactants for the Marcus cross-relation calculations.

DEE reaction	E°, V	ln(A)	λ, eV	r, Å	Z_{red}
$GMP(-H)^{-}$ + $GMP(-H)^{\bullet}$	1.23	31.7	0.82	4.18	-3
$GMPH^{+}$ + $GMPH^{++\bullet}$	1.55	29.2	0.79	4.19	0
$NacTyrO^{-}$ + $NacTyrO^{\bullet}$	0.79	27.0	0.50	3.82	-2
$TyrO^{-}$ + $TyrO^{\bullet}$	0.72	30.2	0.81	3.06	-2
ClO_2^{-} + $ClO_2^{\bullet}$	0.934	28.2	1.53	1.5	-1
N_3^{-} + $N_3^{\bullet}$	1.33	28.2	1.05	2.0	-1
$NO_2^{\bullet}$ + NO_2^{-}	1.04	28.2	1.95	1.9	-1
$[IrCl_6]^{2-}$ + $[IrCl_6]^{3-}$	0.892	28.2	1.04	4.4	-3
$TEMPO^{\bullet}$ + $TEMPO^{+}$	0.745	28.2	0.72	3.67	0

Preprints (www.preprints.org) | NOT PEER-REVIEWED | Posted: 10 August 2023 doi:10.20944/preprints202308.0868.v1

$CysS^- + CysS^\bullet$	0.76	28.2	1.57	3.0	-2
$NacTrpH + NacTrpH^{+\bullet}$	1.15	28.2	0.45	3.83	0

2.6. The T_1 temperature dependence.

The temperature dependences of the nuclear paramagnetic relaxation times T_1 were obtained by means of the CIDNP kinetics simulation. We assume that the main mechanism of relaxation is modulation of the hyperfine interaction (hfi) tensor due to the stochastic rotation of the molecule as a whole. Then the nuclear paramagnetic relaxation time T_1 should depend on the magnetic field B and the rotational correlation time of the molecule as follows:

$$\frac{1}{T_1} \propto \frac{\tau_M}{1+w^2\tau_M^2} \quad (36)$$

If the diffusive stochastic rotation of the radical is fast, $\gamma^2 B^2 \tau_M^2 \ll 1$, then the nuclear paramagnetic relaxation rate $1/T_1$ is proportional to τ_M; the value of τ_M can be estimated from the Stokes-Einstein-Debye equation:

$$\tau_M = \frac{4\pi a^3 \eta}{3kT} \quad (37)$$

According to [51, 52], the temperature dependence of D_2O viscosity in the temperature range 8 - 65ºC is well described by the following equation:

$$\eta(T) = \eta_0 \exp\left(\frac{E}{RT}\right) \quad (38)$$

where E/R = 2059 K, $\eta_0 = 1.14*10^{-6}$ Pa*s.

Then the T_1 temperature dependence should be described by the following equation:

$$T_1(T) = CT\exp\left(-\frac{E}{RT}\right) \quad (39)$$

where C, E/R are parameters, E/R = 2059 K.

The T_1 temperature dependence, Eq. (39) is linearized in the coordinates $\ln(T/T_1)$ vs 1/T (Figure 6).

While fitting by straight lines we discarded by the dropout values. Found values from the slopes of the straight lines E/R are summarized in Table **Error! Reference source not found.**. For 3,5 protons NacTyrO•, 8-th proton GMP(-H)•, H3,4 DPH• protons the slopes coincide within an error with the slope from viscosity dependence. The slope for TyrO• 3,5 protons is almost twice as different from that for viscosity. Earlier we found the slope for the 8-th proton $GMPH^{+\bullet}$, it also coincides with the slope from viscosity dependence.

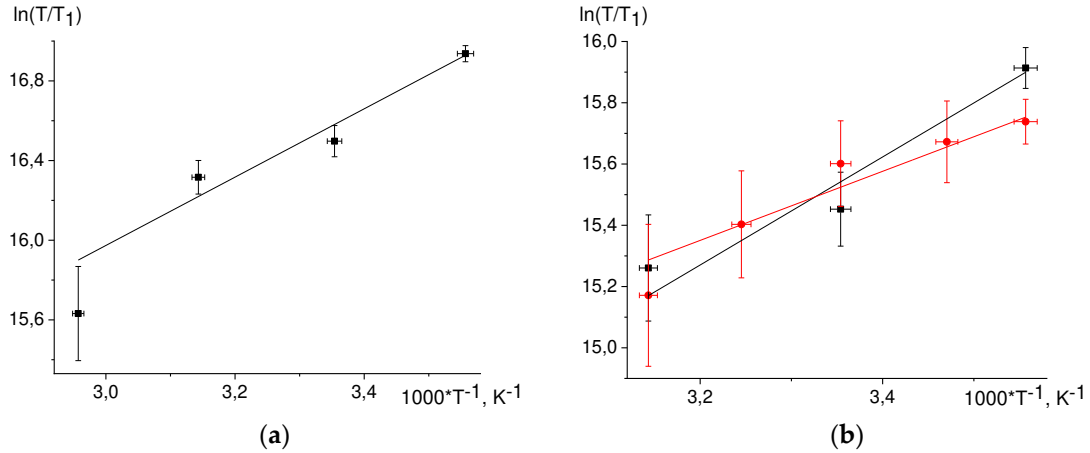

Preprints (www.preprints.org) | NOT PEER-REVIEWED | Posted: 10 August 2023 doi:10.20944/preprints202308.0868.v1

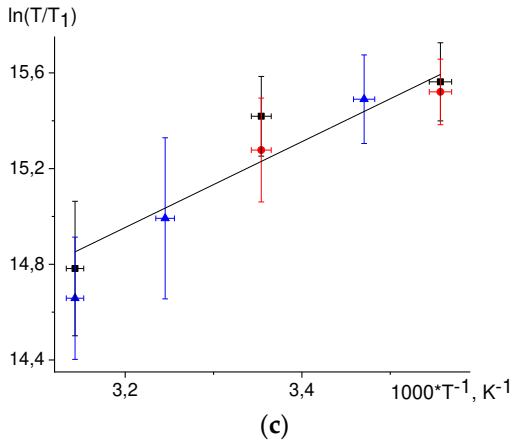

Figure 6. Temperature dependences of the nuclear relaxation time T_1 in coordinates $\ln(T/T_1)$ vs 1/T for: a) H-8 in the radical GMP(-H)• b) H-3,5 in the radical NacTyrO• (black dots) and TyrO• (red dots); c) H-3,4 in the radical DPH• according to the data for systems GMP(-H)$^-$ + DP (black dots), NacTyrO$^-$ + DP (red dots), TyrO$^-$ + DP (blue dots).

Table 6. The energy E values (see Eq. (42)) defined from the linear fitting of $\ln(T/T_1)$ vs 1/T dependencies.

radical, nucleus	**E/R, K**
GMPH^{+}•, H-8 [30]	1993 ± 650
GMP(-H)•, H-8	1720 ± 270
NacTyrO•, H-3,5	1760 ± 370
TyrO•, H-3,5	1130 ± 210
DPH•, H-3,4	1790 ± 300
η(D_2O) [51, 52]	2059 ± 81

For the H-3,5 of NacTyrO•, H-8 of GMP(-H)•, and H-3,4 of DPH• the slopes of the fitted straight lines coincide with the slope for viscosity within an error margin, indicating that rotational modulation of the hfi tensor is the main mechanism of nuclear paramagnetic relaxation of these protons.

The defined energy value E for the 3,5 TyrO• protons is notably different from that for the viscosity dependence. This result can be rationalized assuming that for these protons two mechanisms gives rise to paramagnetic relaxation: modulation of the hfi tensor due to stochastic rotation of the molecule as a whole and modulation of the hfi tensor due to stochastic rotation of the phenolic ring. Assuming that the ring rotation has a small activation energy, the temperature dependence of the correlation time τe for this rotation is as follows:

$$\tau_e = \frac{C}{T} exp\left(\frac{E}{RT}\right) \approx \frac{C_2}{T} \quad (40)$$

while the temperature dependence of the rotational correlation time τ_M is:

$$\tau_M = \frac{C_1}{T} exp\left(\frac{E}{RT}\right) \quad (41)$$

Then the nuclear relaxation time T_1 can be expressed employing Lipari-Szabo [77, 78] equation:

$$\frac{1}{T_1} = C * (S^2\tau_M + (1 - S^2)\tau) \quad (42)$$

$$\tau = \frac{\tau_M\tau_e}{\tau_M+\tau_e} = \frac{C_1}{T} * \frac{exp\left(\frac{E}{RT}\right)*exp\left(\frac{E}{RT_h}\right)}{exp\left(\frac{E}{RT}\right)+exp\left(\frac{E}{RT_h}\right)} \quad (43)$$

where S^2 is an order parameter, playing the role of the dimensionless amplitude of molecular motion: the smaller S^2, the larger the amplitude; T_h is the temperature when the correlation times τ_e and τ_M coincide, $C_2 = C_1 exp(E/(R \cdot T_h))$.

The temperature dependence of the $\ln(T/T_1)$ on 1/T has the form:

Preprints (www.preprints.org) | NOT PEER-REVIEWED | Posted: 10 August 2023 doi:10.20944/preprints202308.0868.v1

$$\ln\left(\frac{T}{T_1}\right) = \ln(C) + \frac{E_n}{RT} + \ln\left(S^2 + (1 - S^2) * \frac{\exp\left(\frac{E}{RT_{half}}\right)}{\exp\left(\frac{E}{RT}\right) + \exp\left(\frac{E}{RT_{half}}\right)}\right) \qquad (44)$$

here E/R = 2059 K is the activation energy for D_2O viscosity. There are three fit parameters: C, S^2, T_h. The value $S^2 = 0.01$ was taken for the fit. The best fit of the experimental data is then achieved at $T_h = 850$ K, see Figure 7.

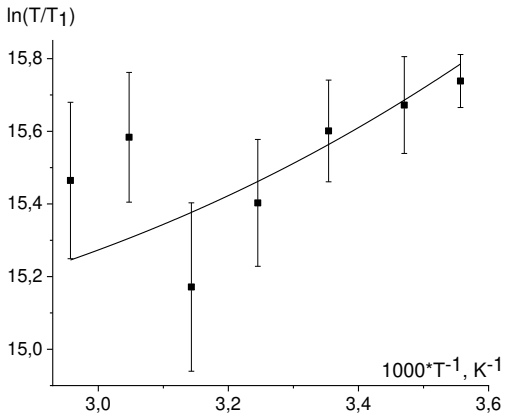

Figure 7. Fitting of the nuclear paramagnetic relaxation temperature dependence of 3,5 protons of radical TyrO• according to the Eq. (44) with a fixed value of $S^2 = 0.01$.

The paramagnetic relaxation time T_1 of the methylene protons (β-CH_2 protons) in the NacTyrO• and TyrO• radicals is almost independent on temperature (Tables **Error! Reference source not found.-Error! Reference source not found.**). We assume that probably the paramagnetic relaxation of β-CH_2 protons occurs also due to the modulation of hfi tensor by intramolecular rotations around the aliphatic bonds. These rotations can have low activation energy, so in a small range of temperatures the rotational frequency changes weakly, which causes the apparent independence of the relaxation time T_1 on the temperature.

3. Discussion

3.1. Comparison of the calculation and experiment

A comparison of the electron transfer reaction rate constants calculated from the Marcus cross relation and those found in the experiment are shown in Table 7 The experimental rate constants were corrected for diffusion by Eq. (30).

Rate constants were calculated by Eq. (34) with parameters from the Table 7. All experimental rate constants were measured at 25°C. We assume that parameters of the dipeptide Gly-TyrO$^-$ do not differ from those of the NacTyrO$^-$ and parameters of the amide N-acetyltyrosine NacTyrO$^-$-NH_2 differ from those of NacTyrO$^-$ only in charge.

Table 7. Comparison of the rate constants calculated from the cross relation and those found in the experiment.

Reaction	k_{12}^{expt}, $M^{-1}s^{-1}$	k_{12}^{calc}, $M^{-1}s^{-1}$	Reference
NacTrpH + $GMPH^{++\bullet}$	$1.2*10^9$	$7.9*10^{10}$	[79]
$TyrO^-$ + GMP(-H)•	$1.7*10^8$	$3.7*10^{10}$	this work
$NacTyrO^-$ + GMP(-H)•	$1.8*10^8$	$1.6*10^{10}$	[29]
$CysS^-$ + GMP(-H)•	$1.9*10^8$	$6.4*10^8$	[80]
$GMP(-H)^-$ + ClO_2•	$1.1*10^5$	$5.6*10^3$	[81]
$GMP(-H)^-$ + N_3•	$3.2*10^9$	$2.0*10^8$	[82]
$TyrO^-$ + ClO_2•	$1.8*10^8$	$1.1*10^8$	[83]
$NacTyrO^-$ + ClO_2•	$7.6*10^7$	$3.2*10^7$	[83]
$TyrO^-$ + N_3•	$6.7*10^9$	$8.1*10^{10}$	[84]

Preprints (www.preprints.org) | NOT PEER-REVIEWED | Posted: 10 August 2023 doi:10.20944/preprints202308.0868.v1

Gly-TyrO$^-$ + $NO_2^\bullet$	$2.0*10^7$	$1.9*10^7$	[85]
NacTyrO-NH_2 + $[IrCl_6]^{2-}$	$3.6*10^7$	$1.2*10^8$	[86]
TEMPO$^\bullet$ + NacTyrO$^\bullet$-NH_2	$1.5*10^8$ [a]	$4.1*10^8$	[87]

[a]the rate constant measured at 22°C.

The agreement with the experiment for reactions involving $GMPH^{+/++\bullet}$, $GMP(-H)^{-/\bullet}$ is noticeably worse than for reactions involving $TyrO^{-/\bullet}$, $NacTyrO^{-/\bullet}$. If GMP is an oxidizing agent, the calculated rate value is overestimated, and when GMP is a reducing agent, the calculated value is underestimated. Perhaps the values of standard potentials for $GMPH^{+/++\bullet}$, $GMP(-H)^{-/\bullet}$ are overestimated, if the error would be in the pre-exponent or in the reorganization energy of GMP, the values would be overestimated or underestimated in all reactions involving GMP, regardless of whether it is oxidation or reduction.

For the reactions TyrO$^-$ + GMP(-H)$^\bullet$, NacTyrO$^-$ + GMP(-H)$^\bullet$ the calculated rate values notably differ from the experimental values than in other GMP involving reactions. Probably this difference can be explained not only by the overestimation of potential of $GMP(-H)^{-/\bullet}$, but also by other causes.

For reactions involving $TyrO^{-/\bullet}$, $NacTyrO^{-/\bullet}$ the calculated values agree well with the experimental values. In the case of the reaction TyrO$^-$ + $N_3^\bullet$, the experimental rate constant is close to the diffusion rate constant; the calculation shows that the reaction occurs in the diffusion control limit; the calculation shows good agreement with the experiment.

3.2. The possible reasons for the failure of the Marcus cross-relation in the reactions of GMP(-H)$^\bullet$ radical reduction by TyrO$^-$, NacTyrO$^-$ anions.

The Marcus cross-relation is fulfilled under the following conditions: the value of ΔG_{12}° is not too large, the reaction is far from the inverted region; the reactants and products are in the ground state; the electron transfer is adiabatic [1, 88]. Also the size difference of the reactants should not be very large ($2\lambda_{12} \approx \lambda_{11} + \lambda_{22}$ requires $2(r_{11}r_{22})^{1/2} \approx r_{11} + r_{22}$), otherwise the expression for the cross relation should be modified [89] .

The Marcus cross-relation for reactions of transition metal complexes was verified in [90-92] and for reactions of organic molecules in [93, 94]. The Marcus cross-relation for redox reactions between organic TMPPD and various inorganic oxidating ions was tested in [95]. A good linear relation over a range of seven orders of magnitudes was found. As a rule, the calculated according to the cross-relation reaction rate constant turns out to be greater than the experimental one; the error increases with the growth of K_{12}. In the above-mentioned works, verification of the cross-relation was done for rate constants measured only at one temperature with the employment of Eqns. (2-4). In these equations, the parameter $\ln(f_{12}) = -(\Delta G_{12}^\circ)^2/(2RT\lambda_{12})$, $f_{12} \approx 1$ at $\Delta G_{12}^\circ \ll \lambda_{12}$. But at large ΔG_{12}° this parameter contributes significantly, and its calculation requires values of the pre-exponents for DEE reactions. In these works, estimates on the order of 10^{11} were taken for the values of the pre-exponents. We believe that this can introduce an error when K_{12} is large. In this work, the values of the pre-exponents and reorganization energies of DEE were determined experimentally; that allows to exclude this error. In particular, it turned out that the pre-exponent in the case of GMP is two orders of magnitude greater than the 10^{11} $M^{-1}s^{-1}$.

In the course of reactions no any isomer product is formed since as it is seen from the CIDNP spectra the electron is transferred only within the aromatic π-systems of the reactants.

When describing the kinetics of electron transfer, the pre-exponent includes the factor κ, which has the meaning of the probability of electron transfer while passing into transition state. For adiabatic reactions κ = 1, the parameter κ is close to unity if there is substantial overlap of the reactant orbitals [96]. For reactions of organic molecules, κ = 1 is usually assumed [93, 97]. In addition, possible nonadiabaticity is taken into account in the cross relation as $\kappa_{12} = (\kappa_{11}\kappa_{22})^{1/2}$.

The steric cross-reacting factor is included in the pre-exponent A_{12} and is estimated as the geometric mean of the steric factors of the DEE, i.e. $A_{12} = (A_{11}A_{22})^{1/2}$.

Another possible reason for the failure of the Marcus cross-relation can be effect of non-electrostatic interactions between the reactants. In the pairs TyrO$^-$/TyrO$^\bullet$, GMP(-H)$^-$/GMP(-H)$^\bullet$, TyrO$^-$

Preprints (www.preprints.org) | NOT PEER-REVIEWED | Posted: 10 August 2023 doi:10.20944/preprints202308.0868.v1

/GMP(-H)• the stacking interactions increasing the stability of pre-reaction complexes are possible. Assume that contribution ΔH^{o} of the stacking-interaction to the enthalpy change of the pre-reaction complex formation is independent of temperature and $\Delta H^{o} < 0$. Then the expressions for the DEE and cross-reaction rate constants taking into account the stacking-interaction are as follows:

$$K_A = K_0 exp\left(\frac{-\Delta H^{\circ} - w_r}{RT}\right) \quad (45)$$

$$k_{11} = K_A^{11} k_{ex} = \frac{A_{11}}{\sqrt{T}} exp\left(\frac{-\Delta H_{11}^{\circ} - w_r}{RT}\right) exp\left(\frac{-\lambda_{11}}{4RT}\right) \quad (46)$$

$$k_{calc}^{red} = \frac{\sqrt{A_{11}A_{22}}}{\sqrt{T}} exp\left(\frac{-\Delta H_{12}^{\circ} - w_{12}}{RT}\right) exp\left(-\frac{(\Delta G_{12}^{\circ} - w_{12} + w_{21} + (\lambda_{11}+\lambda_{22})/2)^2}{2RT(\lambda_{11}+\lambda_{22})}\right) \quad (47)$$

In Eq. (47), we assume that $\Delta H_{12}^{o} \approx \Delta H_{21}^{o}$. The Eq.(46) shows that when treating the temperature dependence of the DEE rate constants by the method described above (i.e. considering only the electrostatic interactions), the found values of the reorganization energies λ_{11}^{obs} will be underestimated: $\lambda_{11}^{obs} = \lambda_{11} + 4\Delta H_{11}^{o}$.

Consideration of the stacking-interaction on the one hand increases the calculated cross-reaction rate constant k_{calc}^{red} due to the factor $\exp(-\Delta H_{12}^{o}/RT)$, on the other hand it decreases, as the calculated reorganization energy increases. The final result depends on the values of ΔH_{11}^{o}, ΔH_{22}^{o}, ΔH_{12}^{o}. When $\Delta H_{11}^{o} = \Delta H_{22}^{o} = \Delta H_{12}^{o} = -RT$ the calculated value of k_{calc}^{red} increases by 1.4 times, when $\Delta H_{11}^{o} = \Delta H_{22}^{o} = -RT$, $\Delta H_{12}^{o} = 0$ it decreases by 2 times.

Marcus cross-relation fails if the electron transfer reaction produces products in the vibrationally-excited state.

When we assume that the overlap of the orbitals in the $TyrO^-$/GMP(-H)• pair is less than in the $TyrO^-$/TyrO•, $GMP(-H)^-$/GMP(-H)• pairs, then the electronic factor of the cross-reaction appears to be less than that calculated from the cross relation, $\kappa_{12} < (\kappa_{11}\kappa_{22})^{1/2}$. The enthalpy of the stacking-interaction for the cross-reaction turns out to be lower than for the DEE reactions. This gives rise to the fact that the cross-reaction rate constant is less than the one we calculated without taking these effects into account.

4. Materials and Methods

The set-up for time-resolved CIDNP experiments was based on a Bruker DRX-200 NMR spectrometer (magnetic field 4.7 Tesla, resonance frequency of protons 200 MHz). A detailed scheme of the setup and methodology of the experiment were published in a review devoted to the application of time-resolved CPNR for studying the kinetics and mechanism of reactions of biologically important molecules [98].

The ^1H CIDNP spectra were recorded as follows. First, the sample in a standard 5 mm NMR Pyrex ampule was barbotaged with argon for 7 min to remove dissolved oxygen. Then, the sample was placed in the NMR spectrometer sensor and broadband homonuclear de-coupler pulses were applied for a few seconds on channel ^1H to suppress the thermal magnetization of the sample. The pulse sequence WALTZ16 was used. The parameters of the sequence were chosen so that the ^1H NMR signals were completely absent from the spectrum without laser irradiation. After that, the sample in the ampoule was irradiated with a single laser pulse of the excimer XeCl-laser COMPEX Lambda Physik (wavelength 308 nm, pulse energy up to 120 mJ, pulse duration ~15 ns), and after time interval τ a registering radiofrequency (RF) pulse with a maximum allowable power -4 dB and duration 1 or 2 μs was applied. After the pulse was applied, the decay of the free induction signal was recorded in the same way as in the conventional NMR experiment. The delay τ was varied in the range from 0 to 100 μs.

The temperature was calibrated by the difference of chemical shifts in the ^1H NMR spectrum of methanol, the temperature measurement error 1K [99].

The pH of the NMR samples was adjusted by addition of NaOD. No correction was made for the deuterium isotope effect on the pH. Experiments with $TyrO^-$ and $NacTyrO^-$ were performed at pH = 11.7, with $GMP(-H)^-$ and $GMP(-H)^-$ + $TyrO^-$ at pH = 11.3. At t = 25ºC the pK_a of phenol groups TyrOH and NacTyrOH are 10.1 and 10.2 [100], pK_a(GMP) = 9.4 [63], pK_a(GMP(-H)•) = 10.8 [64], but deprotonation is slow and the $GMP(-H)^-$ radical is stable at pH = 11.8 for at least 1000 μs [27]. The 2,2'-dipyridyl (DP) was used as a dye (photosensitizer); its concentration was 15 mM in all

Preprints (www.preprints.org) | NOT PEER-REVIEWED | Posted: 10 August 2023 doi:10.20944/preprints202308.0868.v1

experiments. The concentrations of quencher C_q were chosen so that the characteristic quenching time $k_q^{-1}C_q^{-1}$ was shorter than the duration of the recording RF pulse (1-2 μs), and so that a rapid decline in polarization due to too high a product of the observed DEE rate constant and the quencher concentration, $k_{obs}C_q$, was avoided. The compositions of all samples are given in supplementary information.

The GMP in the form of sodium salt hydrate (mass fraction of water 23.4% was determined by ^{1}H NMR), NacTyrOH, TyrOH, D_2O from "Sigma-Aldrich" were used without additional purification, DP was recrystallized from hexane. For the experiment GMP(-H)$^-$ + DP at 65ºC, d8-DP was used because the signals from DP and GMP overlapped each other. The structures of the studied diamagnetic particles GMP(-H)$^-$, NacTyrO$^-$, TyrO$^-$, DP, and the previously studied GMPH$^+$ are shown in Figure 8.

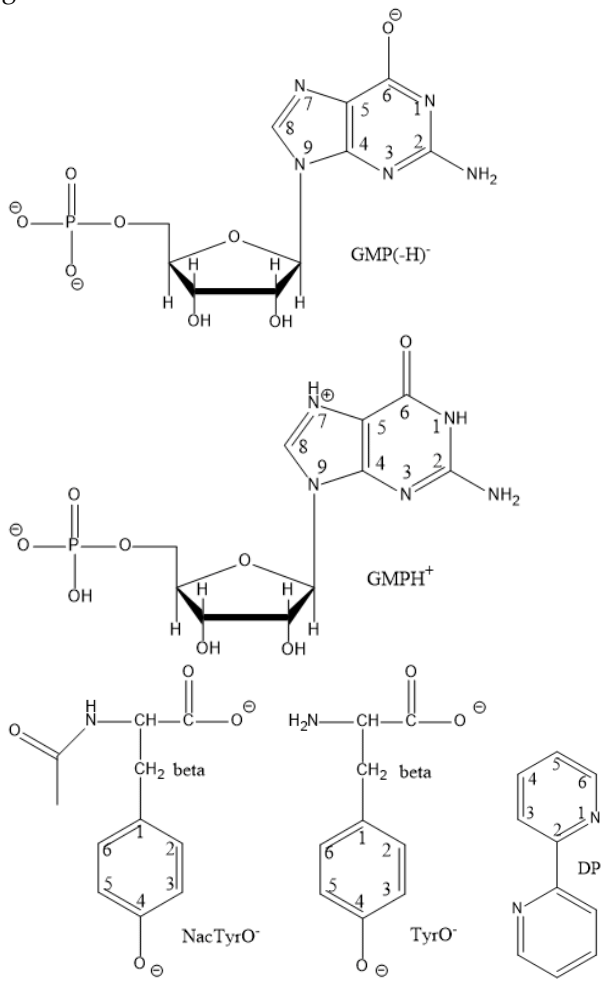

Figure 8. The structures of diamagnetic reactants and products and GMPH$^+$.

At each temperature, two or three kinetic curves differing in the quencher concentration were recorded. To record each kinetic curve, 4 samples were used for the GMP(-H)$^-$ + DP, NacTyrO$^-$ + DP, TyrO$^-$ + DP systems and 8 samples for the GMP(-H)$^-$ + TyrO$^-$ + DP system. Each sample was used twice, the delays were followed in increasing order and in decreasing order to reduce the error from depletion. At each time delay, 4 scans (6 for TyrO$^-$ + DP at 55°C and 65°C) were taken, so each point of the kinetic curve corresponds to 64 signal accumulations for GMP(-H)$^-$ + TyrO$^-$ + DP, 48 signal accumulations for TyrO$^-$ + DP at T = 55°C, 65°C, 32 signal accumulations for GMP(-H)$^-$ + DP, NacTyrO$^-$ + DP, TyrO$^-$ + DP at T = 8-45°C. A 2 μs RF pulse was used for GMP(-H)$^-$ + TyrO$^-$ + DP and TyrO$^-$ + DP at T = 55°C, 65°C; otherwise, a 1 μs RF pulse was used.

All standard electrode potentials E^o used are reported versus NHE.

5. Conclusions.

The CIDNP technique with microsecond time resolution makes it possible to study the kinetics of DEE reactions for the short-lived radicals and determine the DEE reaction rate constant by performing the reaction at different concentrations of the diamagnetic reactant.

The degenerate electron exchange reactions of the neutral radicals GMP(-H)•, TyrO•, NacTyrO• with anions GMP(-H)$^-$, TyrO$^-$, NacTyrO$^-$ in alkaline aqueous media were studied by CIDNP in the temperature range 8-65ºC.

At each temperature chosen in this range, all parameters of CIDNP kinetics were determined, and the experimental values of reorganization energies for the DEE rate constants were found. At the t = 25ºC the rate constant of GMP(-H)• reduction by TyrO$^-$ anion was measured.

The agreement of the calculated rate constants employing Marcus cross relation approach with the experimental ones for the reactions involving GMPH$^{+/++}$•, GMP(-H)$^{-/•}$ is poor, perhaps an overestimated values of the standard electrode potentials for GMPH$^{+/++}$•, GMP(-H)$^{-/•}$ are used.

The rate constants of GMP(-H)• radical reduction by tyrosine and N-acetyltyrosine anions calculated from the cross relation differ by almost two orders of magnitude from those found experimentally, which is a notably greater difference than that for the other reactions involving GMP$^{-•}$ species. Possible causes for this difference are the not taking into account the nonadiabaticity of the cross-reaction and the enthalpy of the stacking interaction between the reactants in the calculation.

At the same time, the calculated rate constants according to the cross-relation of electron transfer reactions involving TyrO$^{-/•}$, NacTyrO$^{-/•}$ coincide well with the literature values.

It was also found that the dependences of the nuclear paramagnetic relaxation rate T_1 on temperature are described by the Arrhenius dependence; for the methylene protons in the tyrosine and N-acetyltyrosine radicals TyrO• and NacTyrO• these dependencies are almost activationless, while for the NacTyrO• 3,5 protons, GMP(-H)• 8-th proton and 3,4 protons of DPH• the activation energy value coincides with the solvent (D_2O) activation energy. This indicates a difference in relaxation mechanisms for these protons: relaxation in the methylene protons of the TyrO• and NacTyrO• radicals occurs due to the modulation of the hfi tensor due to ring inversion, while relaxation in the 3,5 protons of NacTyrO• and 8-th proton of the GMP(-H)• occurs due to modulation of the hfi tensor due to stochastic rotation of the molecule as a whole. The intermediate type of the temperature dependence of the nuclear paramagnetic relaxation rate T_1 is observed for the 3,5 protons of the TyrO• radical: the activation energy was about half the activation energy for the solvent viscosity. We assume that the both relaxation mechanisms manifest themselves in this case.

Author Contributions: : Conceptualization, M.P.G, A.V.Y, G.G, N.N.L.; validation, M.P.G, A.V.Y, G.G, N.N.L..; investigation, O.B.M, A.V.Y, M.P.G; writing— original draft preparation M.P.G, A.V.Y, G.G, N.N.L.; writing— review and editing, M.P.G, A.V.Y, G.G, N.N.L; project administration, A.V.Y. All authors have read and agreed to the published version of the manuscript.

Funding: This research was funded by Ministry of Science and Higher Education of the Russian Federation grant 075-15-2020-779.

Institutional Review Board Statement: Not applicable.

Informed Consent Statement: Not applicable.

Data Availability Statement: Not applicable.

Conflicts of Interest: The authors declare no conflict of interest.

References

1. Marcus, R. A.; Sutin, N., Electron transfers in chemistry and biology. *Biochimica et Biophysica Acta (BBA)-Reviews on Bioenergetics* **1985,** 811, (3), 265-322.
2. Zerk, T. J.; Saouma, C. T.; Mayer, J. M.; Tolman, W. B., Low Reorganization Energy for Electron Self-Exchange by a Formally Copper (III, II) Redox Couple. *Inorganic chemistry* **2019,** 58, (20), 14151-14158.
3. Xie, B.; Wilson, L. J.; Stanbury, D. M., Cross-Electron-Transfer Reactions of the [CuII/I(bite)]2+/+ Redox Couple. *Inorganic Chemistry* **2001,** 40, (14), 3606-3614.

4. Ganesan, M.; Sivasubramanian, V. K.; Rajagopal, S.; Ramaraj, R., Electron transfer reactions of organic sulfoxides with photochemically generated ruthenium(III)–polypyridyl complexes. *Tetrahedron* **2004,** 60, (8), 1921-1929.
5. Meyer, T. J.; Taube, H., Electron-transfer reactions of ruthenium ammines. *Inorganic Chemistry* **1968,** 7, (11), 2369-2379.
6. Dwyer, F. P.; Sargeson, A. M., The Rate of Electron Transfer Between the Tris-(Ethylenediamine)-Cobalt (II) and Cobalt (III) Ions. *The Journal of Physical Chemistry* **1961,** 65, (10), 1892-1894.
7. Krishnamurty, K. V.; Waiil, A. C., Kinetics of the Vanadium(II)-Vanadium(III) Isotopic Exchange Reaction. *Journal of the American Chemical Society* **1958,** 80, (22), 5921-5924.
8. Grampp, G.; Landgraf, S.; Rasmussen, K., Electron self-exchange kinetics between 2,3-dicyano-5,6-dichloro-p-benzoquinone (DDQ) and its radical anion. Part 1. Solvent dynamical effects. *Journal of the Chemical Society, Perkin Transactions 2* **1999**, (9), 1897-1899.
9. Grampp, G.; Rasmussen, K., Solvent dynamical effects on the electron self-exchange rate of the TEMPO/TEMPO^{+} Couple (TEMPO= 2, 2, 6, 6-Tetramethyl-1-Piperidinyloxy Radical) Part I. ESR-Linebroadening measurements at T= 298 K. *Physical Chemistry Chemical Physics* **2002,** 4, (22), 5546-5549.
10. Mladenova, B.; Kattnig, D. R.; Kaiser, C.; Schäfer, J.; Lambert, C.; Grampp, G. n., Investigations of the Degenerate Intramolecular Charge Exchange in Symmetric Organic Mixed Valence Compounds: Solvent Dynamics of Bis (triarylamine) paracyclophane Redox Systems. *The Journal of Physical Chemistry C* **2015,** 119, (16), 8547-8553.
11. Grampp, G.; Mladenova, B. Y.; Kattnig, D.; Landgraf, S., ESR and ENDOR investigations of the degenerate electron exchange reactions of various viologens in solution. Solvent dynamical effects. *Applied Magnetic Resonance* **2006,** 30, (2), 145-164.
12. Chan, M.-S.; Wahl, A. C., Rate of electron exchange between iron, ruthenium, and osmium complexes containing 1, 10-phenanthroline, 2, 2'-bipyridyl, or their derivatives from nuclear magnetic resonance studies. *The Journal of Physical Chemistry* **1978,** 82, (24), 2542-2549.
13. Koval, C. A.; Margerum, D. W., Determination of the self-exchange electron-transfer rate constant for a copper (III/II) tripeptide complex by proton NMR line broadening. *Inorganic Chemistry* **1981,** 20, (7), 2311-2318.
14. Parker, J. F.; Choi, J.-P.; Wang, W.; Murray, R. W., Electron Self-exchange Dynamics of the Nanoparticle Couple [Au25(SC2Ph)18]0/1− By Nuclear Magnetic Resonance Line-Broadening. *The Journal of Physical Chemistry C* **2008,** 112, (36), 13976-13981.
15. Closs, G. L.; Miller, R. J., Laser flash photolysis with NMR detection. Microsecond time-resolved CIDNP: separation of geminate and random-phase processes. *J. Am. Chem. Soc.* **1979,** 101, (6), 1639-41.
16. Closs, G. L.; Miller, R. J.; Redwine, O. D., Time-resolved CIDNP: applications to radical and biradical chemistry. *Acc. Chem. Res.* **1985,** 18, (7), 196-202.
17. Morozova, O. B.; Yurkovskaya, A. V.; Tsentalovich, Y. P.; Forbes, M. D. E.; Hore, P. J.; Sagdeev, R. Z., Time resolved CIDNP study of electron transfer reactions in proteins and model compounds. *Mol. Phys.* **2002,** 100, (8), 1187-1195.
18. Morozova, O. B.; Yurkovskaya, A. V.; Tsentalovich, Y. P.; Forbes, M. D. E.; Sagdeev, R. Z., Time-Resolved CIDNP Study of Intramolecular Charge Transfer in the Dipeptide Tryptophan-Tyrosine. *J. Phys. Chem. B* **2002,** 106, (6), 1455-1460.
19. Goez, M.; Kuprov, I.; Hore, P. J., Increasing the sensitivity of time-resolved photo-CIDNP experiments by multiple laser flashes and temporary storage in the rotating frame. *J. Magn. Reson.* **2005,** 177, (1), 139-145.
20. Morozova, O. B.; Korchak, S. E.; Sagdeev, R. Z.; Yurkovskaya, A. V., Time-Resolved Chemically Induced Dynamic Nuclear Polarization Studies of Structure and Reactivity of Methionine Radical Cations in Aqueous Solution as a Function of pH. *J. Phys. Chem. A* **2005,** 109, (45), 10459-10466.
21. Kuprov, I.; Goez, M.; Abbott, P. A.; Hore, P. J., Design and performance of a microsecond time-resolved photo-chemically induced dynamic nuclear polarization add-on for a high-field nuclear magnetic resonance spectrometer. *Rev. Sci. Instrum.* **2005,** 76, (8), 084103/1-084103/7.
22. Wörner, J.; Chen, J.; Bacher, A.; Weber, S., Non-classical disproportionation revealed by photo-chemically induced dynamic nuclear polarization NMR. *Magn. Reson.* **2021,** 2, (1), 281-290.
23. Pompe, N.; Illarionov, B.; Fischer, M.; Bacher, A.; Weber, S., Completing the Picture: Determination of 13C Hyperfine Coupling Constants of Flavin Semiquinone Radicals by Photochemically Induced Dynamic Nuclear Polarization Spectroscopy. *J. Phys. Chem. Lett.* **2022,** 13, (23), 5160-5167.
24. Goez, M., The Degenerate Electron Exchange between N, N-Dimethylanilines and their Radical Cations. *Zeitschrift für Physikalische Chemie* **1990,** 169, (2), 133-145.
25. Schael, F.; Löhmannsröben, H.-G., The deactivation of singlet excited all-trans-1, 6-diphenylhexa-1, 3, 5-triene by intermolecular charge transfer processes. 1. Mechanisms of fluorescence quenching and of triplet and cation formation. *Chemical physics* **1996,** 206, (1-2), 193-210.

26. Closs, G. L.; Sitzmann, E. V., Measurements of degenerate radical ion-neutral molecule electron exchange by microsecond time-resolved CIDNP. Determination of relative hyperfine coupling constants of radical cations of chlorophylls and derivatives. *J. Am. Chem. Soc.* **1981,** 103, (11), 3217-19.
27. Yurkovskaya, A. V.; Snytnikova, O. A.; Morozova, O. B.; Tsentalovich, Y. P.; Sagdeev, R. Z., Time-resolved CIDNP and laser flash photolysis study of the photoreaction between triplet 2, 2′-dipyridyl and guanosine-5′-monophosphate in water. *Physical chemistry chemical physics* **2003,** 5, (17), 3653-3659.
28. Tsentalovich, Y. P.; Morozova, O. B.; Yurkovskaya, A. V.; Hore, P. J.; Sagdeev, R. Z., Time-Resolved CIDNP and Laser Flash Photolysis Study of the Photoreactions of N-Acetyl Histidine with 2,2'-Dipyridyl in Aqueous Solution. *J. Phys. Chem. A* **2000,** 104, (30), 6912-6916.
29. Morozova, O. B.; Kiryutin, A. S.; Sagdeev, R. Z.; Yurkovskaya, A. V., Electron transfer between guanosine radical and amino acids in aqueous solution. 1. Reduction of guanosine radical by tyrosine. *The Journal of Physical Chemistry B* **2007,** 111, (25), 7439-7448.
30. Geniman, M.; Panov, M.; Morozova, O.; Kiryutin, A.; Fishman, N.; Yurkovskaya, A., Temperature dependence of the degenerate electron exchange between guanosine-5′-monophosphate cation and its short-lived radical dication in aqueous solution. *Russian Chemical Bulletin* **2021,** 70, (12), 2375-2381.
31. Gottlieb, H.; Kotlyar, V.; Nudelman, A., NMR Chemical Shifts of Common Laboratory Solvents as Trace Impurities. *The Journal of organic chemistry* **1997,** 62, 7512-7515.
32. Kaptein, R., Simple rules for chemically induced dynamic nuclear polarization. *J. Chem. Soc., Chem Commun.* **1971**, (14), 732-733.
33. Adhikary, A.; Kumar, A.; Becker, D.; Sevilla, M. D., The Guanine Cation Radical: Investigation of Deprotonation States by ESR and DFT. *The Journal of Physical Chemistry B* **2006,** 110, (47), 24171-24180.
34. Tomkiewicz, M.; McAlpine, R. D.; Cocivera, M., Photooxidation and Decarboxylation of Tyrosine Studied by E.P.R. and C.I.D.N.P. Techniques. *Canadian Journal of Chemistry* **1972,** 50, (23), 3849-3856.
35. Mezzetti, A.; Maniero, A. L.; Brustolon, M.; Giacometti, G.; Brunel, L. C., A tyrosyl radical in an irradiated single crystal of N-acetyl-L-tyrosine studied by X-band cw-EPR, high-frequency EPR, and ENDOR spectroscopies. *The Journal of Physical Chemistry A* **1999,** 103, (48), 9636-9643.
36. Vollenweider, J.-K.; Fischer, H.; Hennig, J.; Leuschner, R., Time-resolved CIDNP in laser flash photolysis of aliphatic ketones. A quantitative analysis. *Chemical physics* **1985,** 97, (2-3), 217-234.
37. Mulazzani, Q. G.; Emmi, S.; Fuochi, P. G.; Venturi, M.; Hoffman, M. Z.; Simic, M. G., One-electron reduction of aromatic nitrogen heterocycles in aqueous solution. 2,2'-Bipyridine and 1,10-phenanthroline. *The Journal of Physical Chemistry* **1979,** 10, 1582-1590.
38. Tsentalovich, Y. P.; Morozova, O. B.; Yurkovskaya, A. V.; Hore, P., Kinetics and Mechanism of the Photochemical Reaction of 2, 2 ′-Dipyridyl with Tryptophan in Water: Time-Resolved CIDNP and Laser Flash Photolysis Study. *The Journal of Physical Chemistry A* **1999,** 103, (27), 5362-5368.
39. Läufer, M., Increasing the time resolution of flash CIDNP by numerical analysis: photoreduction of anthraquinone by N, N-dimethylaniline. *Chemical physics letters* **1986,** 127, (2), 136-140.
40. Goez, M., Evaluation of flash CIDNP experiments by iterative reconvolution. *Chemical Physics Letters* **1990,** 165, (1), 11-14.
41. Morozova, O. B.; Tsentalovich, Y. P.; Yurkovskaya, A. V.; Sagdeev, R. Z., Consecutive biradicals during the photolysis of 2,12-dihydroxy-2,12-dimethylcyclododecanone: low- and high-field chemically induced dynamic nuclear polarizations (CIDNP) study. *J. Phys. Chem. A* **1998,** 102, (20), 3492-3497.
42. Morozova, O. B.; Yurkovskaya, A. V.; Tsentalovich, Y. P.; Sagdeev, R. Z.; Wu, T.; Forbes, M. D. E., Study of Consecutive Biradicals from 2-Hydroxy-2,12-dimethylcyclododecanone by TR-CIDNP, TREPR, and Laser Flash Photolysis. *J. Phys. Chem. A* **1997,** 101, (47), 8803-8808.
43. Morozova, O. B.; Yurkovskaya, A. V.; Tsentalovich, Y. P.; Vieth, H.-M., 1H and 13C Nuclear Polarization in Consecutive Biradicals during the Photolysis of 2,2,12,12-Tetramethylcyclododecanone. *J. Phys. Chem. A* **1997,** 101, (4), 399-406.
44. Tsentalovich, Y. P.; Forbes, M. D. E.; Morozova, O. B.; Plotnikov, I. A.; McCaffrey, V. P.; Yurkovskaya, A. V., Spin and Molecular Dynamics in Acyl-Containing Biradicals: Time-Resolved Electron Paramagnetic Resonance and Laser Flash Photolysis Study. *J. Phys. Chem. A* **2002,** 106, (31), 7121-7129.
45. Tsentalovich, Y. P.; Morozova, O. B.; Avdievich, N. I.; Ananchenko, G. S.; Yurkovskaya, A. V.; Ball, J. D.; Forbes, M. D. E., Influence of Molecular Structure on the Rate of Intersystem Crossing in Flexible Biradicals. *J. Phys. Chem. A* **1997,** 101, (47), 8809-8816.
46. Tsentalovich, Y. P.; Yurkovskaya, A. V.; Sagdeev, R. Z.; Obynochny, A. A.; Purtov, P. A.; Shargorodsky, A. A., Kinetics of Nuclear-Polarization in the Geminate Recombination of Biradicals. *Chem. Phys.* **1989,** 139, (2-3), 307-315.
47. Yurkovskaya, A.; Grosse, S.; Dvinskikh, S.; Morozova, O.; Vieth, H.-M., Spin and molecular dynamics of biradicals as studied by low field nuclear polarization at variable temperature. *J. Phys. Chem. A* **1999,** 103, (8), 980-988.

48. Yurkovskaya, A. V.; Morozova, O. B.; Sagdeev, R. Z.; Dvinskih, S. V.; Buntkowsky, G.; Vieth, H.-M., The influence of scavenging on CIDNP field dependences in biradicals during the photolysis of large-ring cycloalkanones. *Chem. Phys.* **1995,** 197, (2), 157-66.
49. Babenko, S. V.; Kruppa, A. I., Probing the inclusion complexes of short-lived radicals with β-cyclodextrin by CIDNP. *Journal of Inclusion Phenomena and Macrocyclic Chemistry* **2019,** 95, (3), 321-330.
50. Tsentalovich, Y. P.; Morozova, O. B.; Yurkovskaya, A. V.; Hore, P. J.; Sagdeev, R. Z., Time-Resolved CIDNP and Laser Flash Photolysis Study of the Photoreactions of N-Acetyl Histidine with 2,2′-Dipyridyl in Aqueous Solution. *The Journal of Physical Chemistry A* **2000,** 104, (30), 6912-6916.
51. Hardy, R. C.; Cottington, R. L., Viscosity of deuterium oxide and water in the range 5 to 125°C. *J. Res. Natl. Bur. Stand* **1949,** 42, (1934), 573.
52. Nikol'skii, B. P. R. V. A., *Spravochnik khimika [Chemist's Handbook]*. Khimiya: Moscow—Leningrad, 1962; Vol. 1, p 1075.
53. Malmberg, C. G., Dielectric constant of deuterium oxide. *Journal of Research of the National Bureau of Standards* **1958,** 60, (6), 609-612.
54. German, E.; Kuznetsov, A., Outer sphere energy of reorganization in charge transfer processes. *Electrochimica Acta* **1981,** 26, (11), 1595-1608.
55. Shor, N.; Berezovskii, O., Algorithms to construct a minimum-volume invariant ellipsoid for a stable dynamic system. *Cybernetics and Systems Analysis* **1995,** 31, (3), 421-427.
56. Mostad, A.; Rømming, C.; Graver, H.; Husebye, S.; Klæboe, P.; Swahn, C., Crystal-structure of DL-tyrosine. *Acta Chem. Scand* **1973,** 27, 401-410.
57. Emerson, J.; Sundaralingam, M., Zwitterionic character of guanosine 5'-monophosphate (5'-GMP): Redetermination of the structure of 5'-GMP trihydrate. *Acta Crystallographica Section B: Structural Crystallography and Crystal Chemistry* **1980,** 36, (6), 1510-1513.
58. Brunschwig, B. S.; Creutz, C.; Macartney, D. H.; Sham, T.; Sutin, N., The role of inner-sphere configuration changes in electron-exchange reactions of metal complexes. *Faraday Discussions of the Chemical Society* **1982,** 74, 113-127.
59. Harriman, A., Further comments on the redox potentials of tryptophan and tyrosine. *Journal of Physical Chemistry* **1987,** 91, (24), 6102-6104.
60. Mahmoudi, L.; Kissner, R.; Nauser, T.; Koppenol, W. H., Electrode Potentials of l-Tryptophan, l-Tyrosine, 3-Nitro-l-tyrosine, 2,3-Difluoro-l-tyrosine, and 2,3,5-Trifluoro-l-tyrosine. *Biochemistry* **2016,** 55, (20), 2849-2856.
61. Fukuzumi, S.; Miyao, H.; Ohkubo, K.; Suenobu, T., Electron-transfer oxidation properties of DNA bases and DNA oligomers. *The Journal of Physical Chemistry A* **2005,** 109, (15), 3285-3294.
62. Steenken, S.; Jovanovic, S. V., How Easily Oxidizable Is DNA? One-Electron Reduction Potentials of Adenosine and Guanosine Radicals in Aqueous Solution. *J. Am. Chem. Soc.* **1997,** 119, (3), 617-618.
63. Asimov, I., Data for Biochemical Research (Dawson, RMC; Elliott, Daphne C.; Elliott, WH; Jones, KM; eds.). In ACS Publications: 1960.
64. Candeias, L.; Steenken, S., Structure and acid-base properties of one-electron-oxidized deoxyguanosine, guanosine, and 1-methylguanosine. *Journal of the American Chemical Society* **1989,** 111, (3), 1094-1099.
65. Morozova, O. B.; Fishman, N. N.; Yurkovskaya, A. V., Kinetics of reversible protonation of transient neutral guanine radical in neutral aqueous solution. *ChemPhysChem* **2018,** 19, (20), 2696-2702.
66. Saprygina, N. N.; Morozova, O. B.; Abramova, T. V.; Grampp, G. n.; Yurkovskaya, A. V., Oxidation of Purine Nucleotides by Triplet 3, 3′, 4, 4′-Benzophenone Tetracarboxylic Acid in Aqueous Solution: pH-Dependence. *The Journal of Physical Chemistry A* **2014,** 118, (27), 4966-4974.
67. Sun, H.; Oldfield, E., Tryptophan Chemical Shift in Peptides and Proteins: A Solid State Carbon-13 Nuclear Magnetic Resonance Spectroscopic and Quantum Chemical Investigation. *Journal of the American Chemical Society* **2004,** 126, (14), 4726-4734.
68. Stanbury, D. M., Reduction Potentials Involving Inorganic Free Radicals in Aqueous Solution. In *Advances in Inorganic Chemistry*, Sykes, A. G., Ed. Academic Press: 1989; Vol. 33, pp 69-138.
69. Awad, H. H.; Stanbury, D. M., Electron transfer between azide and chlorine dioxide: the effect of solvent barrier nonadditivity. *Journal of the American Chemical Society* **1993,** 115, (9), 3636-3642.
70. Stanbury, D. M.; DeMaine, M. M.; Goodloe, G., Reactive dissolution of nitrogen dioxide in aqueous 15NO2-: the first experimental determination of a main-group electron-exchange rate in solution. *Journal of the American Chemical Society* **1989,** 111, (14), 5496-5498.
71. Margerum, D. W.; Chellappa, K. L.; Bossu, F. P.; Burce, G. L., Characterization of a readily accessible copper(III)-peptide complex. *Journal of the American Chemical Society* **1975,** 97, (23), 6894-6896.
72. Hurwitz, P.; Kustin, K., Kinetic study of the reaction $IrCl_6^{2-}$+ $IrBr_6^{3-}$ ⇌ $IrCl_6^{3-}$+ $IrBr_6^{2-}$. *Transactions of the Faraday Society* **1966,** 62, 427-432.
73. Stanbury, D. M.; Lednicky, L. A., Outer-sphere electron-transfer reactions involving the chlorite/chlorine dioxide couple. Activation barriers for bent triatomic species. *Journal of the American Chemical Society* **1984,** 106, (10), 2847-2853.

74. Hung, M.; Stanbury, D. M., Catalytic and Direct Oxidation of Cysteine by Octacyanomolybdate(V). *Inorganic Chemistry* **2005,** 44, (10), 3541-3550.
75. Gerken, J. B.; Pang, Y. Q.; Lauber, M. B.; Stahl, S. S., Structural Effects on the pH-Dependent Redox Properties of Organic Nitroxyls: Pourbaix Diagrams for TEMPO, ABNO, and Three TEMPO Analogs. *The Journal of Organic Chemistry* **2018,** 83, (14), 7323-7330.
76. Grampp, G.; Rasmussen, K., Solvent dynamical effects on the electron self-exchange rate of the TEMPO˙/TEMPO+ couple (TEMPO = 2,2,6,6-tetramethyl-1-piperidinyloxy radical) Part I. ESR-linebroadening measurements at T = 298 K. *Phys. Chem. Chem. Phys.* **2002,** 4, (22), 5546-5549.
77. Lipari, G.; Szabo, A., Model-free approach to the interpretation of nuclear magnetic resonance relaxation in macromolecules. 1. Theory and range of validity. *J. Am. Chem. Soc.* **1982,** 104, (17), 4546-59.
78. Lipari, G.; Szabo, A., Model-free approach to the interpretation of nuclear magnetic resonance relaxation in macromolecules. 2. Analysis of experimental results. *J. Am. Chem. Soc.* **1982,** 104, (17), 4559-70.
79. Morozova, O. B.; Kiryutin, A. S.; Yurkovskaya, A. V., Electron transfer between guanosine radicals and amino acids in aqueous solution. II. Reduction of guanosine radicals by tryptophan. *The Journal of Physical Chemistry B* **2008,** 112, (9), 2747-2754.
80. Morozova, O. B.; Kaptein, R.; Yurkovskaya, A. V., Reduction of Guanosyl Radical by Cysteine and Cysteine-Glycine Studied by Time-Resolved CIDNP. *The Journal of Physical Chemistry B* **2012,** 116, (28), 8058-8063.
81. Napolitano, M. J.; Stewart, D. J.; Margerum, D. W., Chlorine Dioxide Oxidation of Guanosine 5 '-Monophosphate. *Chemical research in toxicology* **2006,** 19, (11), 1451-1458.
82. Faraggi, M.; Broitman, F.; Trent, J. B.; Klapper, M. H., One-Electron Oxidation Reactions of Some Purine and Pyrimidine Bases in Aqueous Solutions. Electrochemical and Pulse Radiolysis Studies. *The Journal of Physical Chemistry* **1996,** 100, (35), 14751-14761.
83. Napolitano, M. J.; Green, B. J.; Nicoson, J. S.; Margerum, D. W., Chlorine Dioxide Oxidations of Tyrosine, N-Acetyltyrosine, and Dopa. *Chemical Research in Toxicology* **2005,** 18, (3), 501-508.
84. Land, E. J.; Prütz, W., Reaction of azide radicals with amino acids and proteins. *International Journal of Radiation Biology and Related Studies in Physics, Chemistry and Medicine* **1979,** 36, (1), 75-83.
85. Prütz, W. A.; Mönig, H.; Butler, J.; Land, E. J., Reactions of nitrogen dioxide in aqueous model systems: Oxidation of tyrosine units in peptides and proteins. *Archives of Biochemistry and Biophysics* **1985,** 243, (1), 125-134.
86. Song, N. Mechanisms and Kinetics of Proton-Coupled Electron-Transfer Oxidation of Phenols. 2011.
87. Pattison, D. I.; Lam, M.; Shinde, S. S.; Anderson, R. F.; Davies, M. J., The nitroxide TEMPO is an efficient scavenger of protein radicals: Cellular and kinetic studies. *Free Radical Biology and Medicine* **2012,** 53, (9), 1664-1674.
88. Marcus, R. A., Electron transfer reactions in chemistry: theory and experiment (Nobel lecture). *Angewandte Chemie International Edition in English* **1993,** 32, (8), 1111-1121.
89. Weinstock, I. A., Outer-Sphere Oxidation of the Superoxide Radical Anion. *Inorganic Chemistry* **2008,** 47, (2), 404-406.
90. Chou, M.; Creutz, C.; Sutin, N., Rate constants and activation parameters for outer-sphere electron-transfer reactions and comparisons with the predictions of Marcus theory. *Journal of the American Chemical Society* **1977,** 99, (17), 5615-5623.
91. Weaver, M. J.; Yee, E. L., Activation parameters for homogeneous outer-sphere electron-transfer reactions. Comparisons between self-exchange and cross reactions using Marcus' theory. *Inorganic Chemistry* **1980,** 19, (7), 1936-1945.
92. Hupp, J. T.; Weaver, M. J., Electrochemical and homogeneous exchange kinetics for transition-metal aqua couples: anomalous behavior of hexaaquairon(III/II). *Inorganic Chemistry* **1983,** 22, (18), 2557-2564.
93. Eberson, L., Electron-transfer reactions in organic chemistry. In *Advances in physical organic chemistry*, Elsevier: 1982; Vol. 18, pp 79-185.
94. Nelsen, S. F.; Ramm, M. T.; Ismagilov, R. F.; Nagy, M. A.; Trieber, D. A.; Powell, D. R.; Chen, X.; Gengler, J. J.; Qu, Q.; Brandt, J. L.; Pladziewicz, J. R., Estimation of Self-Exchange Electron Transfer Rate Constants for Organic Compounds from Stopped-Flow Studies. *Journal of the American Chemical Society* **1997,** 119, (25), 5900-5907.
95. Grampp, G.; Landgraf, S.; Sabou, D.; Dvoranova, D., Application of Marcus cross-relation to mixed inorganic–organic redox couples. A stopped-flow study of the oxidation of N, N, N′, N′-tetramethyl-p-phenylenediamine with various oxidants. *Journal of the Chemical Society, Perkin Transactions 2* **2002**, (1), 178-180.
96. Sutin, N., Theory of Electron Transfer Reactions: Insights and Hindsights. *Progress in Inorganic Chemistry: An Appreciation of Henry Taube* **1983**, 441-498.
97. Marcus, R., On the theory of oxidation-reduction reactions involving electron transfer. III. Applications to data on the rates of organic redox reactions. *The Journal of Chemical Physics* **1957,** 26, (4), 872-877.

 doi:10.20944/preprints202308.0868.v1

98. Morozova, O. B.; Ivanov, K. L., Time-Resolved Chemically Induced Dynamic Nuclear Polarization of Biologically Important Molecules. *ChemPhysChem* **2019,** 20, (2), 197-215.
99. Raiford, D. S.; Fisk, C. L.; Becker, E. D., Calibration of methanol and ethylene glycol nuclear magnetic resonance thermometers. *Analytical Chemistry* **1979,** 51, (12), 2050-2051.
100. Nelson, D. L.; Lehninger, A. L.; Cox, M. M., *Lehninger principles of biochemistry*. Macmillan: 2008.